Study on CO_2 Removal by Benfield Solution Using FEMLAB

By

ANA FARALIZA BT MOHAMED PUAD

Dissertation submitted in partial fulfillment of
the requirement for the
Bachelor of Engineering (Hons)
(Chemical Engineering)

JANUARY 2005

Universiti Teknologi PETRONAS
Bandar Seri Iskandar
31750 Tronoh
Perak Darul Ridzuan

CERTIFICATE OF APPROVAL

Study on CO_2 Removal by Benfield Solution Using FEMLAB

by

ANA FARALIZA BT MOHAMED PUAD

A project dissertation submitted to the
Chemical Engineering Programme
Universiti Teknologi PETRONAS
In partial fulfillment of the requirement for the
BACHELOR OF ENGINEERING (Hons)
(CHEMICAL ENGINEERING)

Approved by,

(Dr. Suzana Yusup)
Supervisor

UNIVERSITI TEKNOLOGI PETRONAS
TRONOH, PERAK
JANUARY 2005

CERTIFICATION OF ORIGINALITY

This is to certify that I am responsible for the work submitted in this project, that the original work is my own except as specified in the references and acknowledgements, and that the original work contained herein have not been undertaken or done by unspecified source or persons.

ANA FARALIZA MOHAMED PUAD

TABLE OF CONTENTS

ABSTRACT

The main objective of this project is to study CO_2 removal by Benfield solution at various process conditions ie: at various temperature and concentration of lean Benfield solution, at different concentration of diethanolamine (DEA) and at different value of gas mass transfer coefficient, Kg_{CO2}.

Scope of study includes identification of general process description of Benfield absorption system and chemical reactions involved, development of transport phenomena equation that describes Benfield absorption system in mathematical form. Then the required coefficient values are searched through literature review. Followed by modelling using FEMLAB and documentation of FEMLAB output. Finally the results were analyzed and justified with existing studies.

At different temperature of lean Benfield, the rate of CO_2 absorption is increased initially, but further increment of temperature caused less CO_2 to be absorbed. Thus for temperature 333K, 343K and 353K the optimum temperature for this system is found at 343K. The effect of gas mass transfer coefficient, Kg_{CO2} to amount of CO_2 absorption in Benfield solution is inversely proportional. At various concentration of potassium carbonate which are 0.0001 mol/m^3, 0.02 mol/m^3 and 0.06 mol/m^3 the most efficient of CO_2 absorption occurred at 0.02 mol/m^3. The different in concentration of Amine did not affect the system. From the results obtained it can be concluded that the absorption is limited by the resistance to diffusion and finite velocity of the reaction.

ACKNOWLEDGMENT

I would like to express my greatest gratitude to my supervisor, Dr Suzana Yusup for her guidance and readiness to assist throughout the project. I would also like to thank to Dr.Shahidah Mohd Shariff, En. Ariffin Marzuki, En.Shahrul Azman Zainal Abidin and the Process Technology Group of PETRONAS Research & Scientific Services for giving me the opportunity to gain experience and knowledge which is a great assistance in this project throughout my Industrial Internship Programme. My gratitude goes to Final Year Research Project coordinators, Universiti Teknologi PETRONAS (UTP), lecturers and technicians involved in this project. Last but not least, to my beloved parents En.Mohamed Puad bin Yahya and Pn.Jamalia bt Harun and family for their endless support and motivation in any field that I am involved in. Thank you and may Allah bless all of you.

NOMENCLATURE

D_i	Diffusivity of component i in Potassium Carbonate solution (m^2/h)
K	pseudo first order rate constant (h^{-1})
k_{AM}	second order rate costant of amine (m^3/kmol h)
k_{OH}	forward reaction rate constant of reaction (m^3/kmol s)
$k_{\_OH}$	backward reaction rate constant of reaction (s^{-1})
k_g	gas side mass transfer coefficient (kmol/h m^2 atm)
K_g	overall mass transfer coefficient (kmol h^{-1} m^{-2} atm^{-1})
K_1	first ionization constant for carbonic acid (kmol/m^3)
K_2	first ionization constant for carbonic acid (kmol/m^3)
T	gas temperature (K)
t	liquid temperature (K)
N_i	mass transfer flux of i component (kmol/m^2 h)
C_i	Concentration of i species (mol/m^3)

LIST OF FIGURES

LIST OF TABLES

CHAPTER 1
INTRODUCTION

1.1 PROJECT BACKGROUND

Control of Carbon Dioxide (CO_2) in hydrocarbon gas from the gas wells is important because of the long distances the gas pipelines run to the customers. Significant levels of CO_2 add cost to the compression and transport of the gas. CO_2 also causes problems by lowering the hydrate icing temperature of the gas causing major potential problems in its compression.

One particular CO_2 removal process technology is the Benfield Process, which uses potassium bicarbonate to remove the CO_2 in the form of potassium carbonate. Benfield process or also known as hot carbonated process was originally developed by Benson et al. [1], and has since undergone several improvement [2-4]. The most important improvement is the discovery that small amount of certain organic additives (promoters) can enhance the absorption rate largely [5].

Benfield solution is a mixture of 30% potassium carbonate solution, is dosed with 3% DEA (Diethyl Amine) and up to 200 ppm of antifoam, to improve solution characteristics, with 0.5% of Vanadium Pentoxide to inhibit corrosion. [18]

1.2 PROBLEM STATEMENT

In Hysys Steady State Simulation, the Benfield model for PETRONAS Gas Processing Plant-3 (GPP3) can not be developed accurately because of the limiting factor in the property package. The published information investigated the modeling and simulation of Benfield process is very little. In this project, further study was done in order to identify the effect of different parameters on the performance of the absorption system using FEMLAB. General model of CO_2 absorption by Benfield solution in falling film that investigated the combination effect of mass transfer and chemical reaction has been developed.

1.3 OBJECTIVE

The objective of this project is to study the CO_2 absorption from natural gas at various operating condition of Benfield solution. The study will focus on the effect of CO_2 exit concentration profile:

i. At various temperature in the range of 333K to 353K and concentration of Benfield solution in the range of 0.0001 mol/m^3 to 0.06 mol/m^3.

ii. At various concentration of DEA in the range of 0.00001mol/m^3 to 0.002mol/m^3 in Benfield solution.

iii. At different value of CO_2 gas mass transfer coefficient, $KgCO_2$ in the range of 0.3 to 0.7 kmol h^{-1} m^{-2} atm^{-1}

1.4 SCOPE OF WORK

The scopes of work for this study are as follow:

- Identify general process description of Benfield absorption system and chemical reactions involved.
- Develop the best transport phenomena equation that describe the Benfield absorption system in mathematical form.
- Search on required coefficient value.
- Perform modeling using FEMLAB
- Documentation of FEMLAB output.
- Results analysis and justification with existing studies.

1.4.1 Relevancy of the Project

The separation of carbon dioxide from mixtures with other gases is a process of substantial industrial importance. Through modeling, the degree of the effectiveness of Benfield system to remove CO_2 from natural gas can be visualized. Thus, knowing CO_2 level in the gas at various points in a removal train allows large savings in operating costs. Optimization of the operation of each plant would yield CO_2 concentrations within specification but with minimal utilities and raw material usage. In this project, CO_2 absorption process incorporated with chemical reactions are fully integrated with transport phenomena with the aid of Finite Element Modelling.

CHAPTER 2
LITERATURE REVIEW

2.1 Gas Treating Process

Gas treating process variables such as solvent type and concentration, pressure and circulation can be manipulates to produce specification quality hydrocarbon products. Interest has increased recently in exploring the effects of inlet gas and solvent temperatures as an aid in meeting these specifications. In general, lower temperature tend to promote absorption of lower molecular weight components based on vapour-liquid equilibrium.

Physical solvents exploit this principle by absorbing acid gases and water at lower temperatures. However, if the reaction is kinetically limited as is the case with CO_2 and Benfield solution, it is impossible to determine how temperature affects the absorption in the absence of additional information. This ambiguity results from the competing phenomena and opposite effect temperature has on reaction rates and solubility [14].

For gas treating, process performance is often defined relative to the ability of a solvent to absorb one component to a greater degree than another. This is often referred as "selectivity". For Benfield solution (chemical solvent), selectivity may occur due to reaction kinetics. In this case, selectivity may be dramatically improved by column operating temperature [14].

There is no sharp dividing line between pure physical absorption and absorption controlled by the rate of chemical reaction. Most cases fall in optimum value in which the rate of absorption is limited both by the resistance to diffusion and by finite velocity of the reaction [12].

2.2 FUNDAMENTALS OF CHEMICAL SOLVENT

Chemical solvents use the same premise as physical solvents to absorb the component into solution. However, the chemical solvent now has the ability to change the absorbed component either by causing it to ionize or to transform into another component by chemical reaction involved. In either case, the absorbed component in solution is depleted by this reaction, resulting the ability of the solvent to absorb more of the component from the gas phase. This process continues until chemical and physical equilibrium is reached. Contact time in the absorber might prevent the attainment of equilibrium conditions depending on the rate of the reaction.[14].

2.3 FUNDAMENTALS OF CHEMICAL REACTION

Reactions are governed by equilibrium constants, which are related to the Gibbs free energy. The reaction proceeds to a minimum in the Gibbs free energy. The equilibrium constant is used to determine the concentration of species at equilibrium at a given temperature and an initial feed. Large equilibrium constants results in larger concentrations of the products. Theoretically, more acid gas could be absorbed at higher temperature based solely on the equilibrium constants. However, the chemical reaction of the acid gas is not the only process occurring. The absorption of acid gas is less at higher temperatures for equilibrium processes due to primarily to the decrease in solubility [14].

The rate at which a chemical reaction happens is described by kinetics. If a chemical reaction is kinetically limited, then the reaction may not be necessarily approach equilibrium. A reaction that is thermodynamically possible but for which no reasonably rapid mechanism is available is said to be kinetically limited. The extent to which the

reaction approaches equilibrium depends on the time allowed to react, the temperature and the driving forces or concentrations [14] .

2.4 REACTION KINETICS

The basic reaction chemistry for aqueous hot potassium carbonate solution and CO_2 is represented by the following reversible reaction [8]:

$$CO_2 + K_2CO_3 + H_2O \leftrightarrow 2KHCO_3 \qquad (1)$$

Since potassium carbonate and bicarbonate are both strong electrolytes, it may be assumed that the metal is present only in the form of K+ ions, so reaction (1) may be more realistically represented in the ionic terms as:

$$CO_2 + CO_2^{-3} + H_2O \leftrightarrow 2HCO^{-3} \qquad (2)$$

The above reaction is evidently made up of a sequence of elementary steps. The carbonate ion first reacts with water to generate hydroxyl ions, which then react with CO_2 as follows [8]:

$$CO_2^{-3} + H_2O \leftrightarrow HCO^{-3} + OH^- \qquad (3)$$

$$CO_2 + OH^- \leftrightarrow HCO^{-3} \qquad (4)$$

Since reaction (3) is instantaneous reaction, reaction (4) is the rate-controlling step, so that the rate equation for reaction of carbon dioxide with un-promoted hot potassium carbonate leads to [8,14]:

$$r_{OH} = k_{OH}[OH^-][CO_2] - k_{-OH}[HCO^{-3}] \qquad (5)$$

where k_{OH} and k_{-OH} are forward and backward rate constants of reaction (4).At equilibrium condition Eq. (5) gives:

$$k_{-OH}[HCO^{-3}] = k_{OH}[OH^-][CO_2]_e \qquad (6)$$

where $[CO_2]e$ is the equilibrium concentration of CO_2. The expression for reverse reaction (4) in Eq. (6) has been evaluated by considering conditions at equilibrium, but it is generally true, even when the system is not at equilibrium [14–16].Substituting Eq. (6) into Eq. (5) gives [14]:

$$r_{OH} = (k_{OH}[OH^-])\,([CO_2] - [CO_2]_e) \qquad (7)$$

Carbonate–bicarbonate system is a buffer solution, so the concentration of OH− ion in the solution near the surface of liquid is not significantly depleted by the absorbed CO_2. In this case, the carbon dioxide undergoes a pseudo-first order reaction and Eq. (7) may be rewritten as [8,14,15]:

$$r_{OH} = k1([CO_2] - [CO_2]_e) \qquad (8)$$

where k1 denotes apparent first-order rate constant.

When a small amount of amine is added into the solution, the absorption rate of carbon dioxide is enhanced greatly according to the following reactions [8]:

$$CO_2 + RR\_NH \leftrightarrow RR\_NCOOH \qquad (9)$$

(Amine) (Carbamate)

$$RR\_NCOOH + OH^- \leftrightarrow HCO^{-3} + RR\_NH \qquad (10)$$

(Carbamate) (Amine)

At higher temperatures in the range of industrial operating conditions, the rate of reaction (10) increases significantly, system is better represented by the homogeneous catalysis mechanism [15,8], and reaction (9) is rate-controlling step. Using the same approach for deriving Eq. (8), gives the following pseudo-first order rate equation for rAm [14]:

$$r_{Am} = (kAm[Am])([CO_2] - [CO_2]_e) = k2([CO_2] - [CO_2]e) \qquad (11)$$

where k2 is apparent first-order rate constant.

Adding Eqs. (7) and (11) leads to the overall pseudo-first order rate equation of carbon dioxide with promoted hot potassium carbonate in liquid phase:

$$r = (kOH[OH^-] + kAm[Am])([CO_2] - [CO_2]_e)$$

$$= k([CO_2] - [CO_2]_e) \qquad (12)$$

where k is the overall apparent first-order rate constant and is defined as:

$$k = (kOH[OH^-] + kAm[Am]) \qquad (13)$$

2.5 MASS TRANSFER

The combined effect of chemical reaction presented by Eq. (12) and mass transfer are conveniently and adequately treated by the framework of penetration-surface renewal theory developed by Danckwerts [14]. The absorption rate of carbon dioxide in the liquid phase according to this theory nd homogeneous catalysis mechanism can be expressed as follows [14–16]:

$$N_{CO2} = EkL(CCO2i - CCO2e) \quad (24)$$

where CCO2i is the concentration of carbon dioxide at the interface and CCO2e is the equilibrium concentration of unreacted carbon dioxide in the bulk of liquid when the reverse reaction of carbon dioxide is appreciable. kL is liquid phase mass transfer coefficient and E is the enhancement factor and describes the mass transfer coupled by chemical reactions as follows [14]:

$$E = [1 + (DCO_2k/ k_L^2)]^{0.5} \quad (25)$$

where k is defined by Eq. (13).The rate of absorption, which is defined by Eq. (24), can be rewritten in terms of physical solubility of carbon dioxide in solution, H, in the reactive K_2CO_3 solution as:

$$N_{CO2} = k_LHE(P_{CO2i} - P_{CO2e}) \quad (26)$$

The rate of mass transfer of carbon dioxide in the gas phase is also as follows:

$$N_{CO2} = kg_{CO2} (P_{CO2} - P_{CO2i}) \quad (27)$$

where kg_{CO2} is gas phase mass transfer coefficient of carbon dioxide.

Combining Eqs. (26) and (27) and eliminating the interface partial pressure of carbon dioxide, P_{CO2i}, gives rise to the following equation for the absorption rate:

$$N_{CO2} = [\, kg_{CO2}\, kLEH / (kg_{CO2} + kLEH)\,]\, (P_{CO2} - P_{CO2e})$$

$$= Kg_{CO2} (P_{CO2} - P_{CO2e}) \quad (28)$$

where Kg_{CO2} is overall gas phase mass transfer coefficient of carbon dioxide.

CHAPTER 3
METHODOLOGY

3.1 Simulation Strategy and Model Development

The simulation strategies involve the development of transport phenomena equations, and simplification of chemical reactions equations for the absorption system. The purpose of simulation strategies is to describe the system in mathematical form, which then exported to the FEMLAB programme for model development.

3.1.1 Transport Phenomena Equations

The model threats a falling film, measuring absorption of $CO_{2\,(g)}$ in Benfield solution. The solution provides the concentration process of 6 species in the system.

Assumptions that made in order to simplify the model are:

i. Condensation and evaporation of water in the system will not take into account.
ii. Neglect homogeneous gas reactions
iii. The flow in liquid phase is laminar
iv. The radius of the tube is large enough, in comparison to the thickness of the falling film. Thus the effect of curvature in the tube can be neglected.
v. The contribution of diffusion to the flux of species is negligible in the direction of convective flow i.e. in vertical direction.
vi. The system is isothermal.

The chemical species that are modelled are tabulated below:

Table 3.1.1: Modelled Chemical Species

INDEX (i)	1	2	3	4	5	6
SPECIES	CO_2	OH^-	HCO_3^-	CO_3^{2-}	DEA	Carbamate

Momentum Balance gives the velocity profile v_y :

$v_y = 1.5\ v_{av}(\ 1 - (x/\delta)^2)$

The space coordinate x is 0 at the gas phase boundary and δ at the wall of the tube. The coordinate y is 0 at the inlet and equal to the length of the tube at the outlet.

For mass balance the general expression for the flux vector of every species:

$Ni = (-Di\ \partial c_i / \partial x,\ c_i v_y)$ in Ω where i = 1,2,3,4,5.6

Mass balance incorporates with chemical reactions at steady state for the species:

$Ni - \Sigma R_j = 0$ in Ω where i = 1,2,3,4,5,6

The equation above can be expressed in the following form:

$-Di\ (\partial^2 c_i / \partial x^2) + v_y(\partial c_i / \partial y) - \Sigma R_j = 0$ in Ω where i = 1,2,3,4,5,6

This equation can be rewrite by using the transformation $y = v_{av}\, t$.

This gives the final system of equation in the domain:

$(1.5\ (1 - (x/\delta)^2))\ \partial c_i / \partial t - Di\ (\partial^2 c_i / \partial x^2) - \Sigma R_j = 0$ in Ω where i = 1,2,3,4,5,6

This transformation implies that the boundary conditions at y=0 become initial conditions. This gives the following initial conditions:

$C_i(x,0) = 0$

$C_2(x,0) = C_{OH}$

$C_3(x,0) = C_{HCO3-}$

$C_4(x,0) = C_{CO32-}$

$C_5(x,0) = C_{DEA}$

$C_6(x,0) = C_{CARB}$

The corresponding boundary conditions:

$-D_i (\partial c_i / \partial x)(0,t) = 0$ for i = 2,3,4,5,6

$-D_1 (\partial_1 / \partial x)(0,t) = kg\ CO_2 (P_{CO2} - P_{CO2eqb})$

Boundary condition at the tube wall:

$-D_i (\partial_i / \partial x)(\delta,t)$ for i = 1,2,3,4,5,6

Which implies that there is no flux of species out of domain at this boundary.

3.1.2 Chemical Reactions Equations

In order to observe the concentration distribution of each ion in this system, rate of reactions in equation 2,3,4,9,10 are estimated as follows:

k2, k3 = kOH

k_2, k_3= k_OH

k4, k5 = kAM

k_4,k_5= k_AM

By assuming reaction (2) made up of a sequence of elementary steps which is reaction (3) and reaction (4). Reaction (3) is instantaneous reaction and reaction (4) is the rate-controlling step Thus reaction rate constant for reaction (2) is estimated as equal with kOH. The same goes with reaction rate constant for reaction (3). (for forward reaction)

For Amine-CO_2 reaction, it is assumed that reaction (9) is rate-controlling step.
Thus, the forward reaction rate constant for equation (9) and equation (10) are approximated equal with kAM.

Where:

Log (kOH) = (13.635 – (2895/T) + 0.081)/ 3600

kAM= 6.4×10^8 exp (14.97x (1-(353/T))

K1 = kOH / k_OH

K2 = kAM/ k_AM

The reaction rate expressions for every species are tabulated in the Table 3.12.

Table 3.1.2: Reaction Rate Expression for Modelled Chemical Species

Species	Reaction Rate Expression
CO_2	r_{CO2} = -kOH[CO_2][OH^-]+k_OH [HCO_3^-]-kAM[CO_2][DEA]-k_AM [CARB]
OH^-	rOH= kOH [CO_3^{2-}]-k_OH[HCO_3^-][OH^-]-k OH[CO_2][OH^-] +k_OH[HCO_3^-]-kAM[CARB][OH]+ k_AM[HCO_3^-][DEA]
HCO_3^-	rHCO_3-=kOH[CO_3^{2-}]-k_OH[HCO_3^-][OH^-]+kOH[CO_2][OH^-]-k_OH[HCO_3^-] +kAM[CARB][OH] -k_AM[HCO_3^-][DEA]
CO_3^{2-}	r$CO_3$2-= -kOH[CO_3^{2-}]+k_OH[HCO_3^-][OH^-]
DEA	rDEA=-kOH[CO_2][DEA]+k_AM[CARB]+kAM[CARB][OH^-]-k_AM[HCO_3^-][DEA]
Carbamate	rCARB= kAM[CO_2][DEA]-k_AM[CARB]-kAM[CARB][OH^-]+k_AM [HCO_3^-][DEA]

3.1.3 FEMLAB Modeling

The system is modelled using the FEMLAB Graphical User Interface. The modelling procedures are:

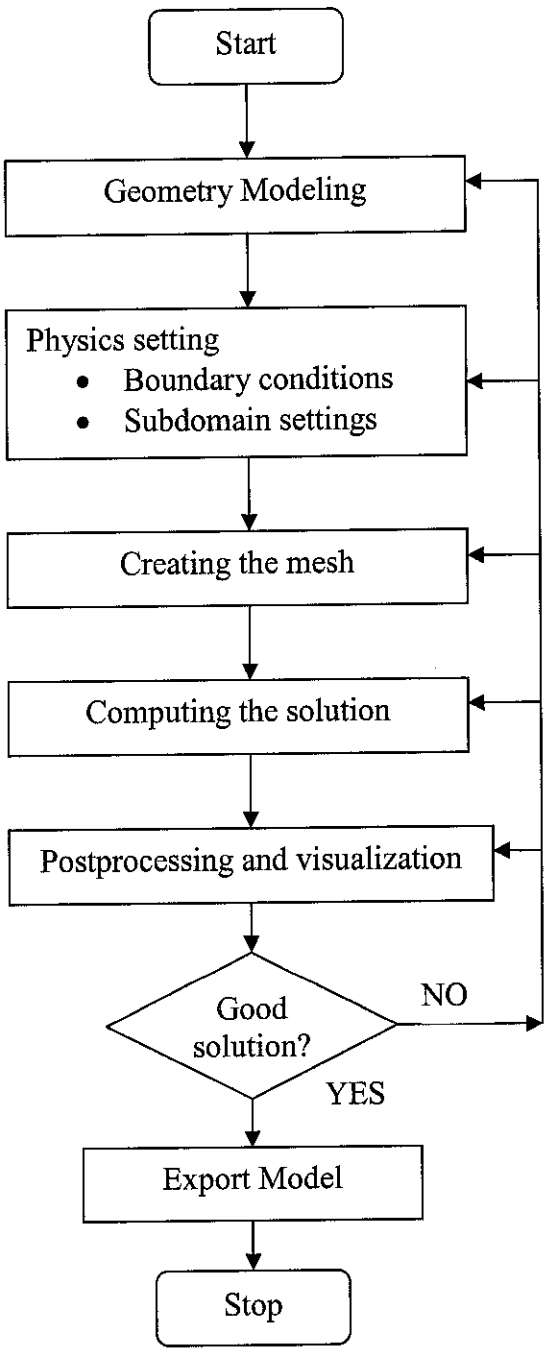

Figure 3.13: Step by Step of FEMLAB Modeling

CHAPTER 4
RESULTS AND DISCUSSION

4.1 FEMLAB Program

Nine FEMLAB program was run to simulate the CO_2 absorption by Benfield solution. The concentration profiles of CO_2 at the top of the column are observed and will be discussed in this chapter at various temperature and concentration of Benfield solution, at various concentration of DEA and at various value of CO_2 gas mass transfer coefficient, Kg_{CO2}.

Run 1, Run 2 and Run 3 simulate the system at different temperature which are 343K. 333K and 353K respectively. While Run 3, Run 4 and Run 5 showed the effect of different value of CO2 mass transfer coefficient, $KgCO_2$. The effects of Potassium Carbonate concentration in Benfield solution are simulated in Run 5, Run 6 and Run 7. Finally Run 7, Run 8 and Run 9 simulate the effect of promoter concentration to the absorption system. All of these can be achieved by changing the variable as desired. Table 4.1 shows the input of the program.

Table 4.1: Program Input Data

Variable	RUN 1	RUN 2	RUN 3	RUN 4	RUN 5	RUN 6	RUN 7	RUN 8	RUN 9
T (K)	343	333	353	353	353	353	353	353	353
Vav (m/s)	0.0362	0.0362	0.0362	0.0362	0.0362	0.0362	0.0362	0.0362	0.0362
D1 (m^2/h)	6.7e-6	5e-9	5e-4	5e-4	5e-4	5e-4	5e-4	5e-4	5e-4
D2 (m^2/h)	6.4e-9	6e-12	6e-7	6e-7	6e-7	6e-7	6e-7	6e-7	6e-7
D3 (m^2/h)	4.5e-9	4e-12	4e-7	4e-7	4e-7	4e-7	4e-7	4e-7	4e-7
D4 (m^2/h)	5e-7	5e-9	3.5e-5	3.5e-5	3.5e-5	3.5e-5	3.5e-5	3.5e-5	3.5e-5
D5 (m^2/h)	3.35e-5	4e-8	3.35e-4	3.35e-4	3.35e-4	3.35e-4	3.35e-4	3.35e-4	3.35e-4
D6 (m^2/h)	3.35e-5	4e-8	3.35e-4	3.35e-4	3.35e-4	3.35e-4	3.35e-4	3.35e-4	3.35e-4
K_{OH} (s^{-1})	1.9e5	1.05e5	3.27e5	3.27e5	3.27e5	3.27e5	3.27e5	3.27e5	3.27e5
K_{AM}(m^3/kmol h)	4.14e8	2.6e8	6.4e8	6.4e8	6.4e8	6.4e8	6.4e8	6.4e8	6.4e8
K_1(kmol/m^3)	4.43e-7	5e-7	4.198e-7	4.198e-7	4.198e-7	4.198e-7	4.198e-7	4.198e-7	4.198e-7
K_2(kmol/m^3)	7.46e-11	7.189e-11	7.49e-11	7.49e-11	7.49e-11	7.49e-11	7.49e-11	7.49e-11	7.49e-11
CCO2 (mol/m^3)	0.00	0.00	0.00	0.00	0.00	0.00	0.00	0.00	0.00
COH (mol/m^3)	0.02	0.02	0.02	0.02	0.02	0.02	0.02	0.02	0.02
CHCO3 (mol/m^3)	0	0	0	0	0	0	0	0	0
CCO32 (mol/m^3)	0.02	0.02	0.02	0.02	0.02	0.0001	0.06	0.06	0.06
DEA (mol/m^3)	0.002	0.002	0.002	0.002	0.002	0.002	0.002	0.00001	0.001
PCO2 (atm)	0.5	0.5	0.5	0.5	0.5	0.5	0.5	0.5	0.5
PCO2eqb (atm)	0.05	0.05	0.05	0.05	0.05	0.05	0.05	0.05	0.05
Kg_{CO2} (kmol h^{-1} m^{-2} atm^{-1})	0.5	0.5	0.5	0.7	0.3	0.3	0.3	0.3	0.3
Delta (m)	0.1	0.1	0.1	0.1	0.1	0.1	0.1	0.1	0.1

4.2 Discussion

4.2.1 Effect of Liquid Temperature

Inlet temperature of lean solution has an influence on the absorption performance. The effect of Benfield solution inlet temperature to the concentration of CO_2 at the top of the column can be viewed in Figure 4.2.1. The liquid temperatures are varied at 333K, 343K and 353K. Initially by increasing the temperature, the absorption rate is increased, but further increment of temperature caused less CO_2 to be absorbed.

Clearly observed that the concentration of CO_2 is the smallest which is 0.7mol/m^3 at 343K. Temperature 333K and 353K gives 0.94 mol/m^3 and 0.93 mol/m^3 of CO_2 at the top outlet of the column respectively.

Theoretically, higher mass-transfer performance at lower temperature, which can be presented by decreasing the equilibrium vapour pressure of CO_2 over the portion of solution last contacted by gas. Meanwhile more acid gas could be absorbed at higher temperature, if equilibrium constant is based solely. However, the chemical reaction of the acid gas is not the only process occurring in Benfield absorption system.

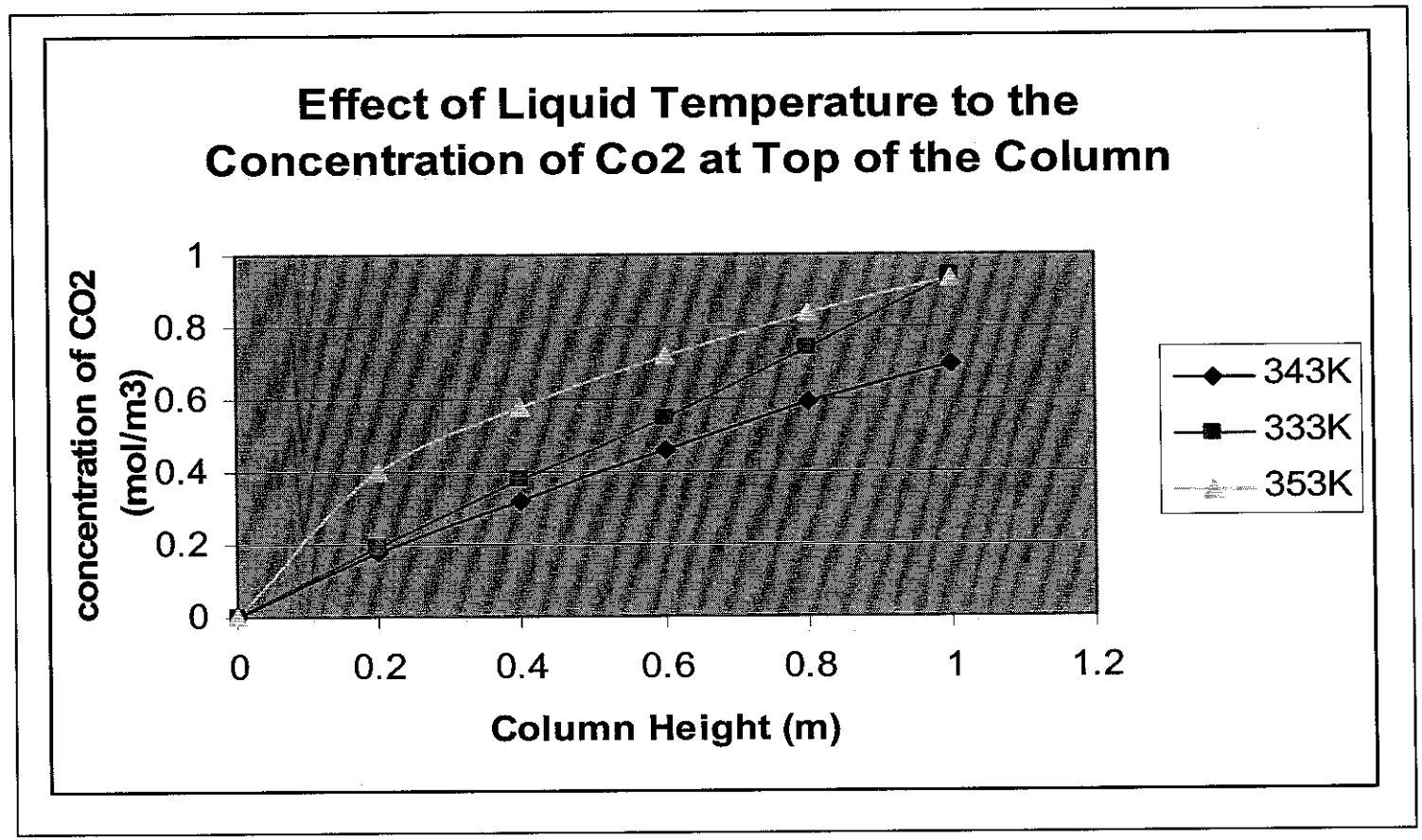

Figure 4.2.1: Effect of Liquid Temperature to the CO_2 Concentration at Top of the Column

4.2.2 Effect of Potassium Carbonate Concentration

In this project, the effect of Potassium Carbonate concentration in Benfield solution are represented by the concentration of carbonate ion (CO_3^{2-}) Three different value of CO_3^{2-} concentrations are simulated and the effect to the CO_2 concentration at top of the column are observed.

The CO_3^{2-} concentrations are varied at 0.02mol/m^3, 0.001mol/m3 and 0.06mol/m^3. The results show that the concentration of CO_2 is the smallest which is 0.58mol/m^3 at optimum CO_3^{2-} concentration, 0.02mol/m^3. CO_3^{2-} concentration 0.001mol/m^3 and 0.006 mol/m^3 gives 0.94 mole/m^3 and 0.93 mol/m^3 of CO_2 at the top outlet of the column respectively.

Concentration is the driving force for absorption to occur. When the different in concentration of Potassium Carbonate solution with CO_2 is high, it is predicted that more CO_2 will be absorbed due to higher solubility of CO_2. The mass transfer is not the only process occurring. The absorption in Benfield system is dramatic between chemical reactions involved and the mass transfer. Thus, it can be concluded that the absorption will be efficient at optimum value of Potassium Carbonate concentration.

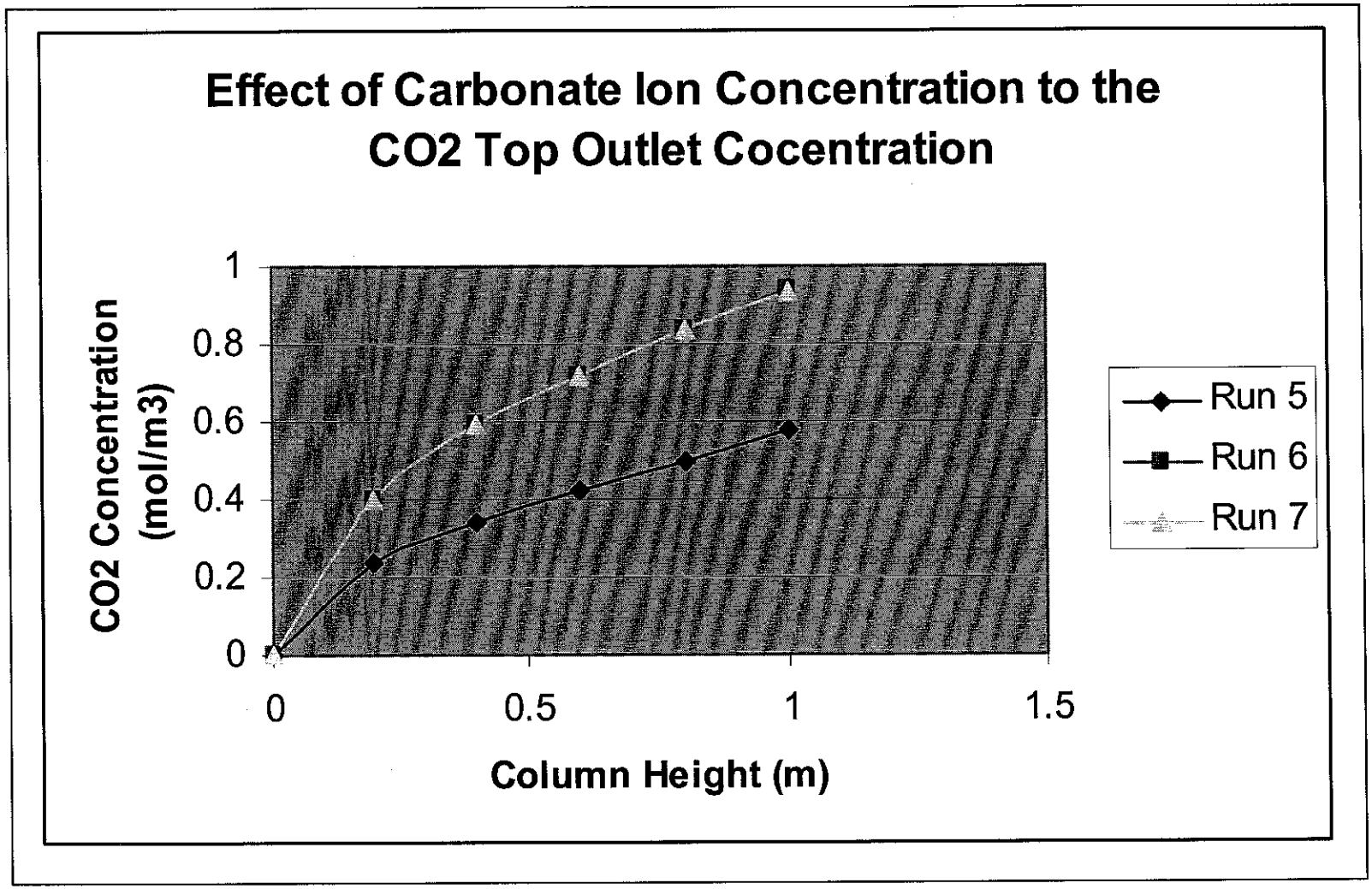

Figure 4.2.2: Effect of Carbonate Ion Concentration to the CO_2 Concentration at the Top Outlet of the Column

4.2.3 Effect of Promoter Concentration

Figure 4.2.3 shows that the changes in Amine concentration did not effect the concentration of CO_2 at the top of the column. Theoretically an increase in the amine concentration first induces a higher CO_2 removal while raising the amine content beyond a specific amount has no effect on the exit CO_2 concentration. The possible explanation for this behaviour is that increasing the amine concentration reflects the higher enhancement factor in the liquid phase, which is directly proportional to the overall Kg in the case of liquid-phase controlled mass transfer. With more increasing the amine concentration, the gas phase mass transfer is considered the major factor controlling the absorption process so the CO_2 removal is unaffected by increasing the amine concentration.

Theoretically water is another component which substantially transported in gas phase across the interface. It may be assumed that there is no liquid-side resistance for the mass transfer of the solvent water vapour. Therefore, the overall mass transfer coefficient for water vapour is the same as the mass transfer coefficient in gas phase. In this project, the term of liquid –phase mass transfer coefficient did not introduced to the simulator. this is because in the model assumptions it already stated that the condensation and evaporation of water in the system did not take into account. This justify why the system did not effected by changing the Amine concentration.

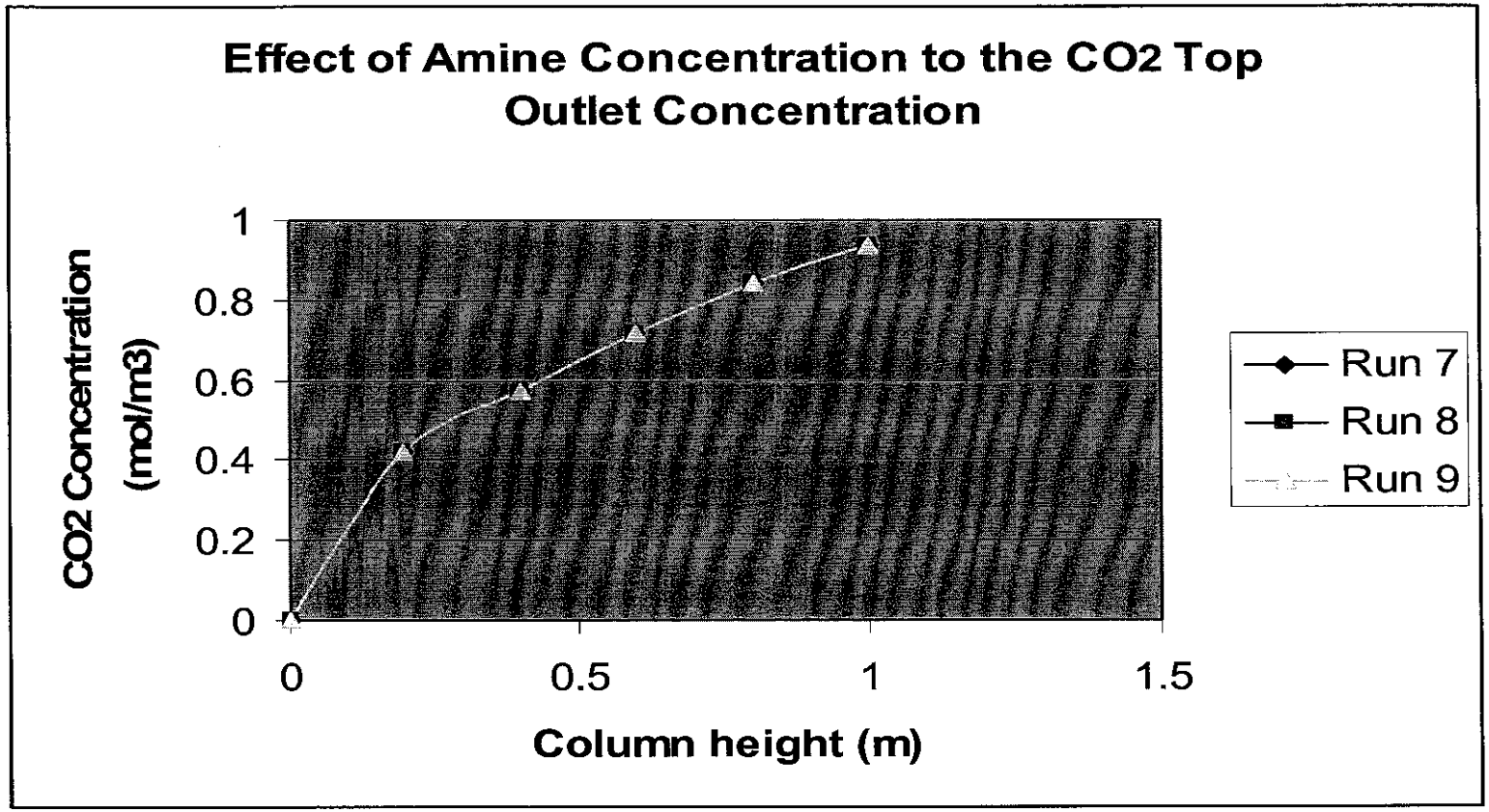

Figure 4.2.3 : Effect of Amine Concentration to the CO_2 Concentration at Top of the Column.

4.2.4 Effect of Gas Mass Transfer Coefficient, $KgCO_2$.

The effect of gas mass transfer coefficient, $KgCO_2$ to the concentration of CO_2 at the top of the column can be viewed in Figure 4.2.4. The values of $KgCO_2$ are varied at 0.5, 0.7 and 0.3 $mol.h^{-1}m^{-2}atm^{-1}$. Clearly observed that the concentration of CO_2 is the smallest which is 0.58 mol/m^3 at smallest value of $KgCO_2$, 0.3 $mol.h^{-1}m^{-2}atm^{-1}$. $KgCO_2$ 0.5, 0.7 $mol.h^{-1}m^{-2}atm^{-1}$ gives 0.9 $mole/m^3$ and 1.26 mol/m^3 of CO_2 at the top outlet of the column respectively. The results showed that as $KgCO_2$ value is decreased, the absorption of CO_2 will be efficient.

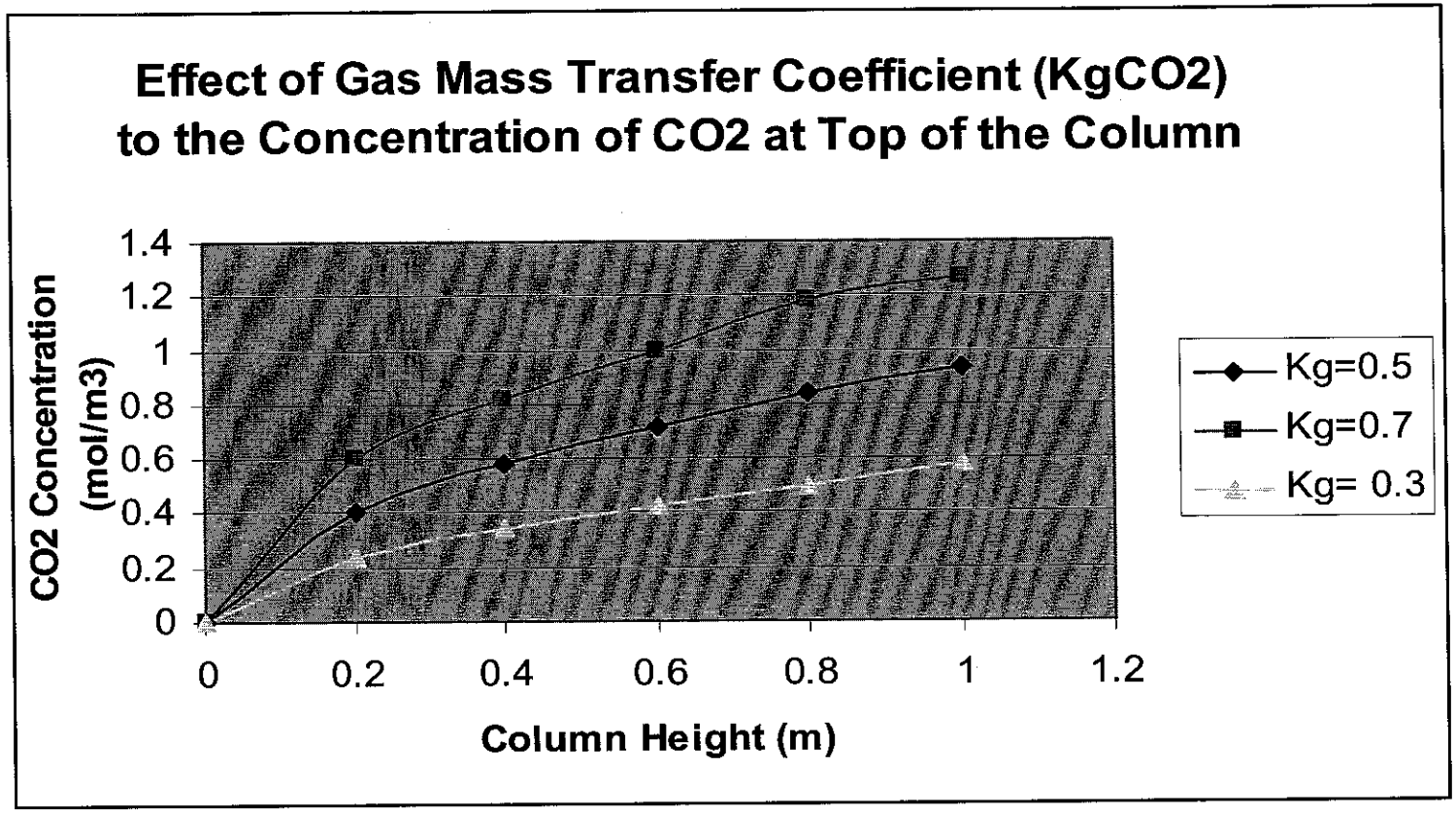

Figure 4.2.4: Effect of Gas Mass Transfer Coefficient (Kg_{CO2}) to the Concentration of CO2 at Top of the Column.

CHAPTER 5
CONCLUSION AND RECOMMENDATIONS

5.1 CONCLUSION

This study has been conducted due to very little detailed of published information that investigated the modelling and simulation of Benfield absorption system. FEMLAB model of CO_2 absorption by Benfield solution in falling film has been developed using mass transport properties and equations of chemical reactions. The model was run at various operating conditions to observe the effect of CO_2 concentration at top outlet of the column.

At different temperature of lean Benfield, the absorption rate of CO_2 is increased initially, but further increment of temperature caused less amount of CO_2 could be absorbed. Thus for temperature 333K, 343K and 353K the optimum temperature for this system is found at 343K.

The effect of gas mass transfer coefficient, Kg_{CO2} to amount of CO_2 absorption in Benfield solution is inversely proportional.

At various concentration of potassium carbonate which are 0.0001 mol/m^3, 0.02 mol/m^3 and 0.06 mol/m^3 the most efficient of CO_2 absorption occurred at 0.02 mol/m^3.

The different in concentration of Amine did not affect the system.

From the results obtained it can be concluded that the absorption is limited by the resistance to diffusion and finite velocity of the reaction.

5.2 RECOMMENDATIONS

In order to improve the project, it would be recommended to include the heat balance in the modelling system. In this case study, due to lack of information the heat balance cannot be incorporated in the system. Since this study already provides the fundamentals of Benfield absorption, it is suggested in the next level, focus will be more on estimation of constants value. Due to time constraints the constant values are only approximated.

CHAPTER 6
REFERENCES

[1] H.E. Benson, J.H. Field, R.M. Jimson, CO_2 Absorption Employing Hot Potassium Carbonate Solution, Chem. Eng. Prog. 50 (1954) 356–364.

[2] H.E. Benson, J.H. Field, W.P. Haynes, Improved Process for CO_2 Absorption Using Hot Carbonate Solution, Chem. Eng. Prog. 52 (1956) 433–438.

[3] H.E. Benson, J.H. Field, New data for hot carbonate process, Petrol. Refinery 39 (1960) 127–132.

[4] H.E. Benson, R.W. Parish, Improved Benfield Process, Hydrol. Process. 53 (4) (1974) 81–88.

[5] F.C. Riesenfield, J.F. Mullowney, Giammarco–Vetrocoke Processes, Petrol. Refinery 38 (5) (1959) 161–167.

[6] G. Astarita, D.W. Savage, Promotion of CO_2 Mass Transfer in Carbonate Solutions, Chem. Eng. Sci. 36 (1981) 581–588.

[7] P.V. Danckwerts, Gas–Liquid Reactions, McGraw-Hill, 1970.

[8] P.V. Danckwerts, M.M. Sharma, The Absorption of Carbon Dioxide Into Solutions of Alkalis and Amines, Chem. Eng. 44 (1966) 244–280.

[9] E. Leder, The absorption of CO_2 Into Chemically Reactive Solutions at High Temperature, Chem. Eng. Sci. 26 (1971) 1381–1390.

[10] M.R.Rahimpour, A.Z Kashooli, Enhanced Carbon Dioxide Removal by Promoted Hot Potassium Carbonate in a Split-Flow Absorber, Chemical Engineering and Processing 43 (2004) 857-865.

[11] J.Tim Cullinane, Gary T.Rochelle, Carbon Dioxide Absorption with Aqueous Potassium Carbonate Promoted by Piperizine, Chemical Engineering Science 59 (2004) 3619-3630.

[12] Robert H.Perrry, Don W.Green, Perry's Chemical Engineers' Handbook, Seventh Edition,McGraw Hill (1998) 5_69-5_71.

[13] Octave Levenspiel, Chemical Reaction Engineering, Third Edition,John Wiley & Sons, (1999).

[14] Kevin Lunsford, Gavin Mcintyre, Decreasing Contactor Temperature Could Increase Performance, Bryan Research & Engineering (2001).

[15] PFK Project, Traning Textbook for Ammonia and Methanol Units Operation, Part1, Mitsubisi Heavy Industries,LTD,MCEC. 1998.

APPENDICES

4.1.1 Run 1, Run 2 and Run 3 Results

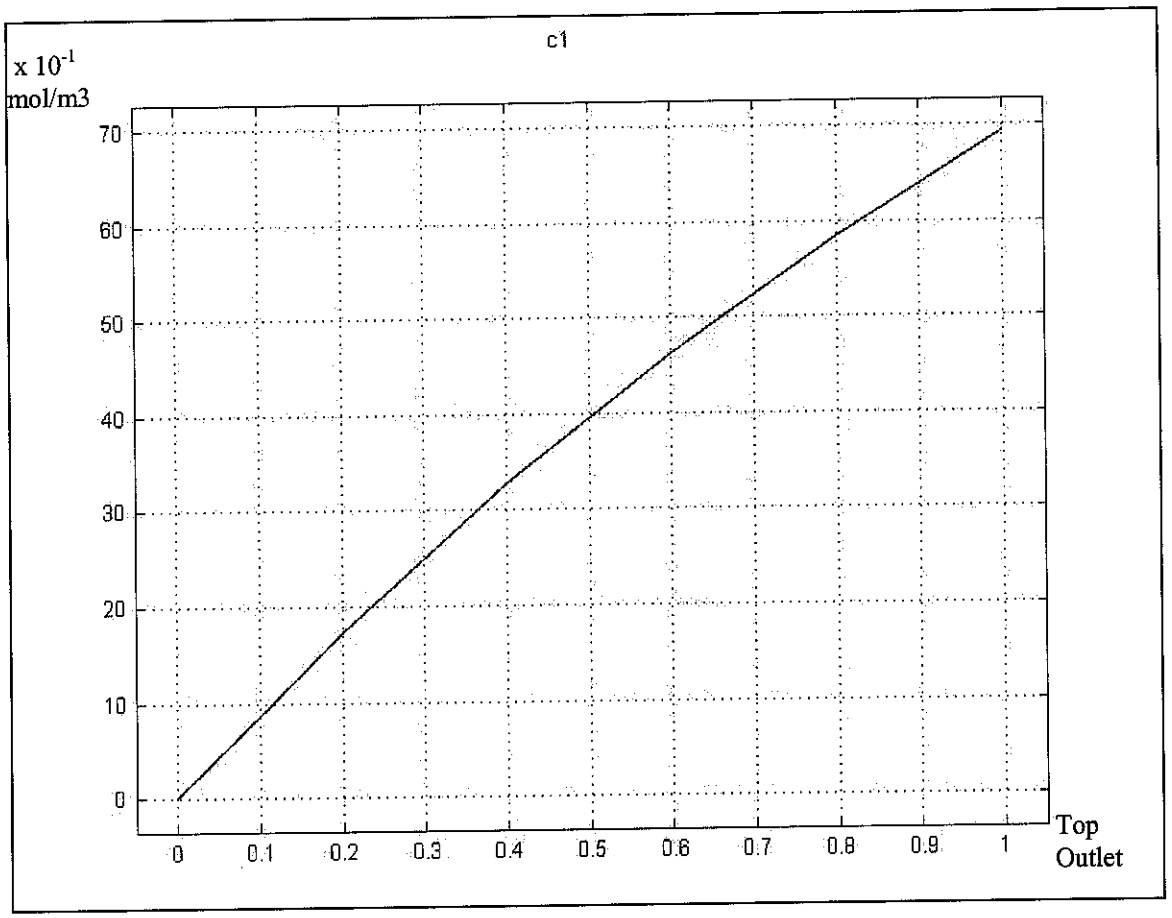

Figure 4.1.1a: Concentration profile of CO_2 absorbed at 343K (Run 1)

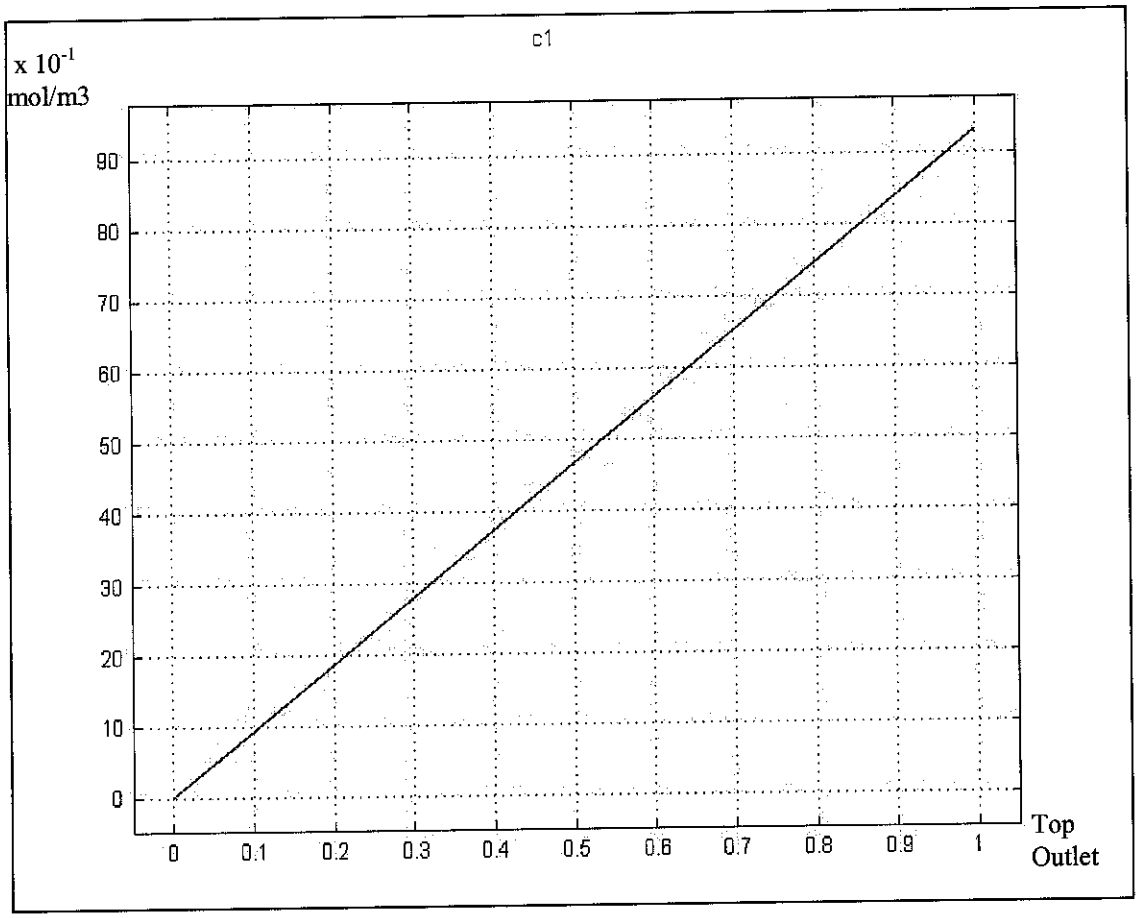

Figure 4.1.1b: Concentration profile of CO_2 absorbed at 333K (Run 2)

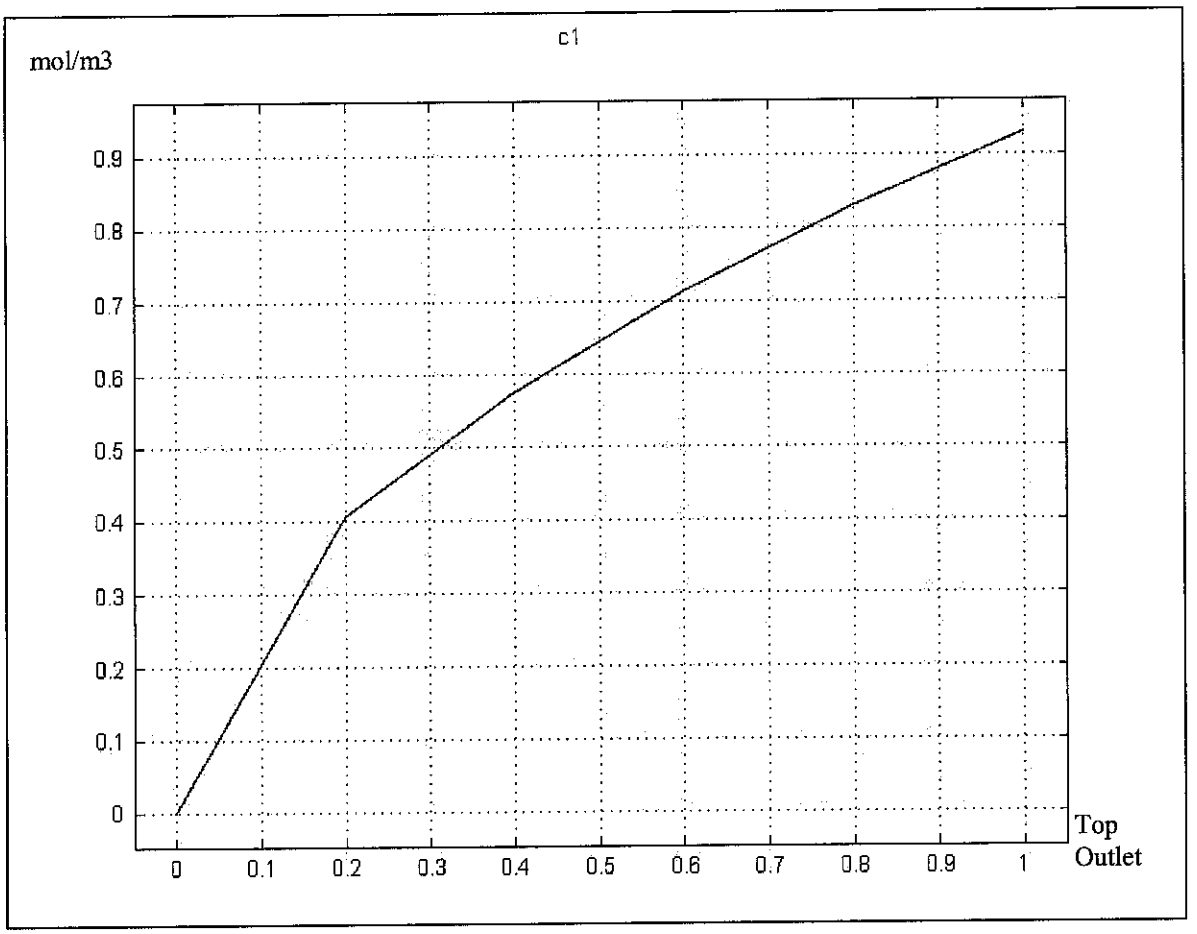

Figure 4.1.1c: Concentration profile of CO_2 absorbed at 353K (Run 3)

4.1.2 Run 3, Run 4 and Run 5 Results

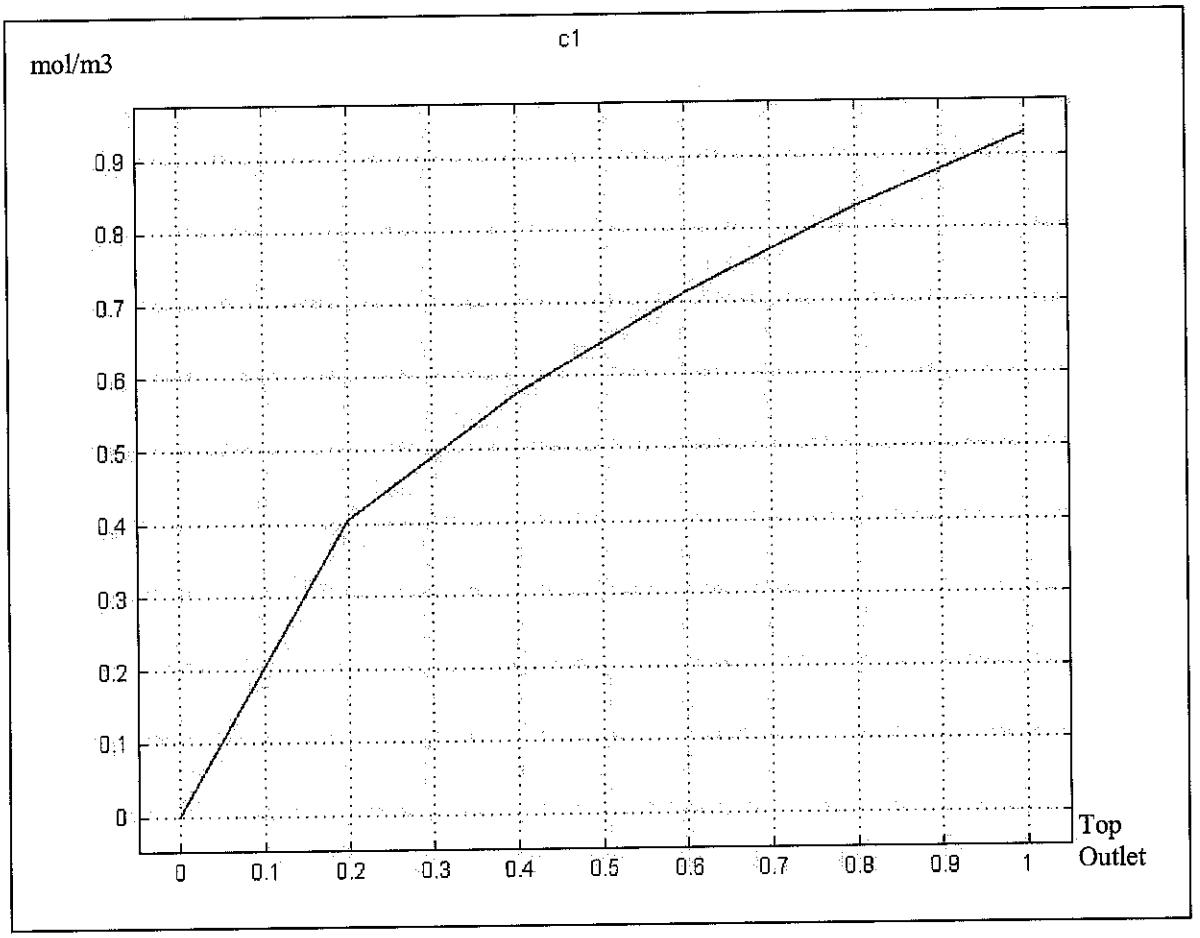

Figure 4.1.2a: Concentration profile of CO_2 absorbed at Kg_{CO2} 0.5 $mol.h^{-1}m^{-2}atm^{-1}$ (Run 3)

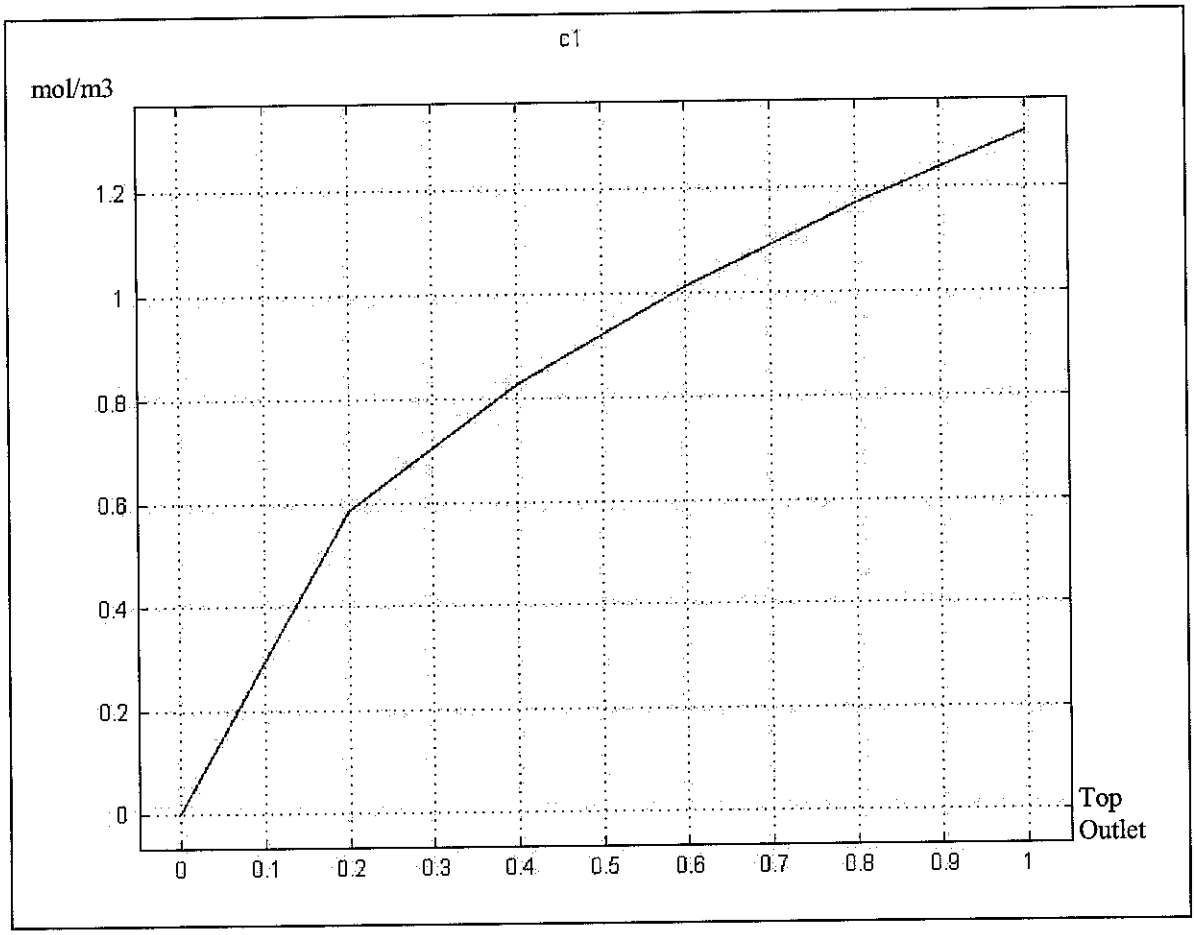

Figure 4.1.2b: Concentration profile of CO_2 absorbed at Kg_{CO2} 0.7 $mol.h^{-1}m^{-2}atm^{-1}$ (Run 4)

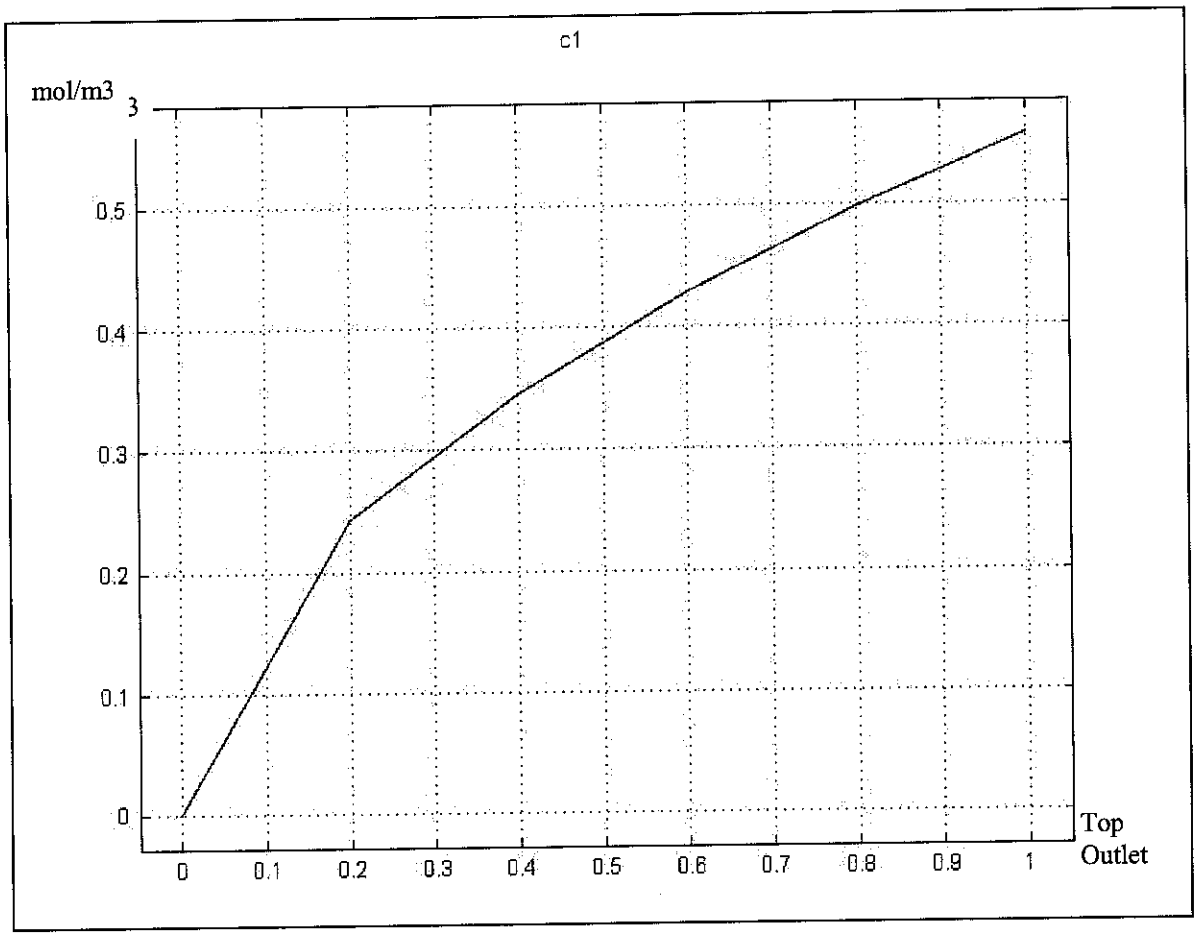

Figure 4.1.2c: Concentration profile of CO_2 absorbed at Kg_{CO2}=0.3mol.h^{-1}m^{-2}atm^{-1} (Run 5)

4.1.3 Run 5, Run 6 and Run 7 Results

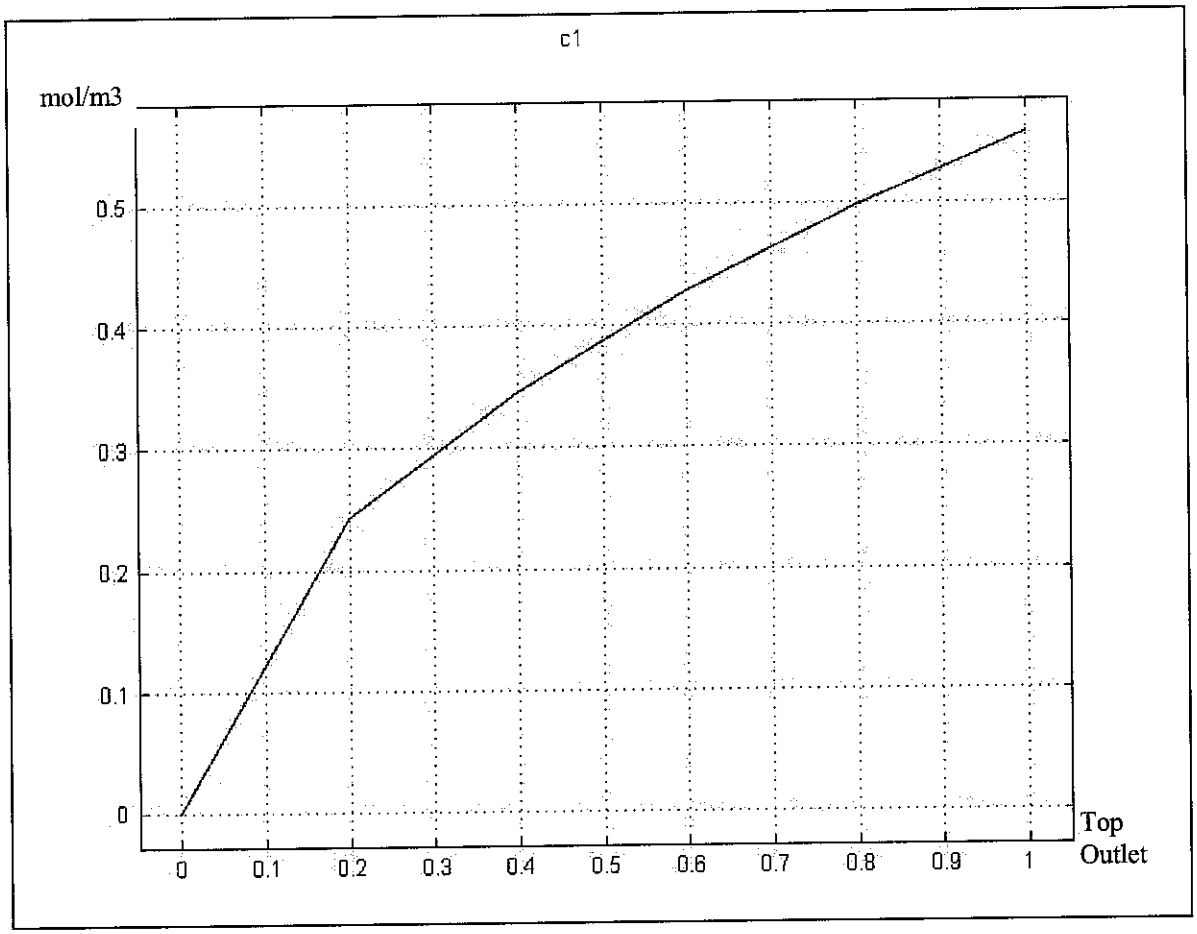

Figure 4.1.3a: Concentration profile of CO_2 absorbed at Concentration of CO_3^{2-} = 0.02 mol/m^3.(Run 5)

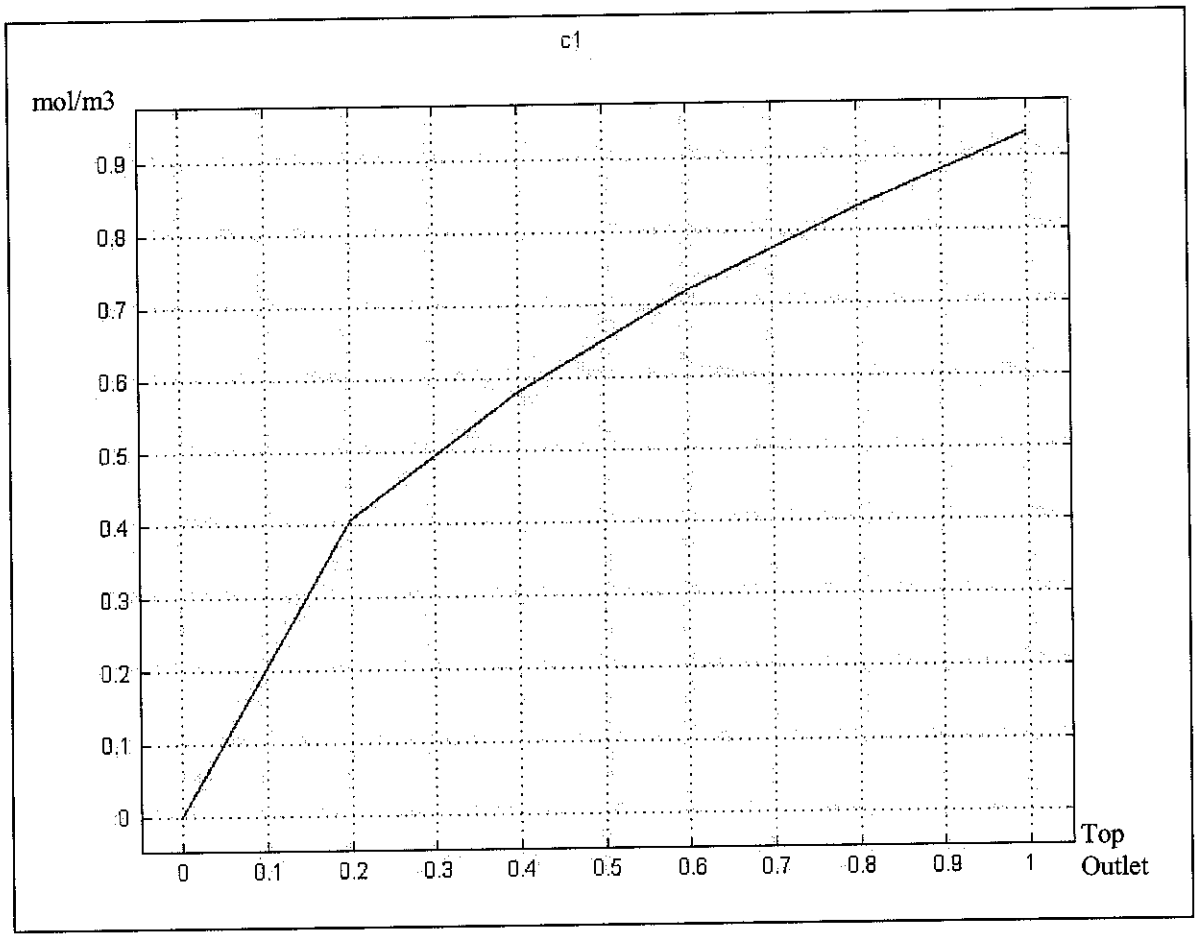

Figure 4.1.3b: Concentration profile of CO_2 absorbed at Concentration of CO_3^{2-} = 0.0001 mol/m^3. (Run 6)

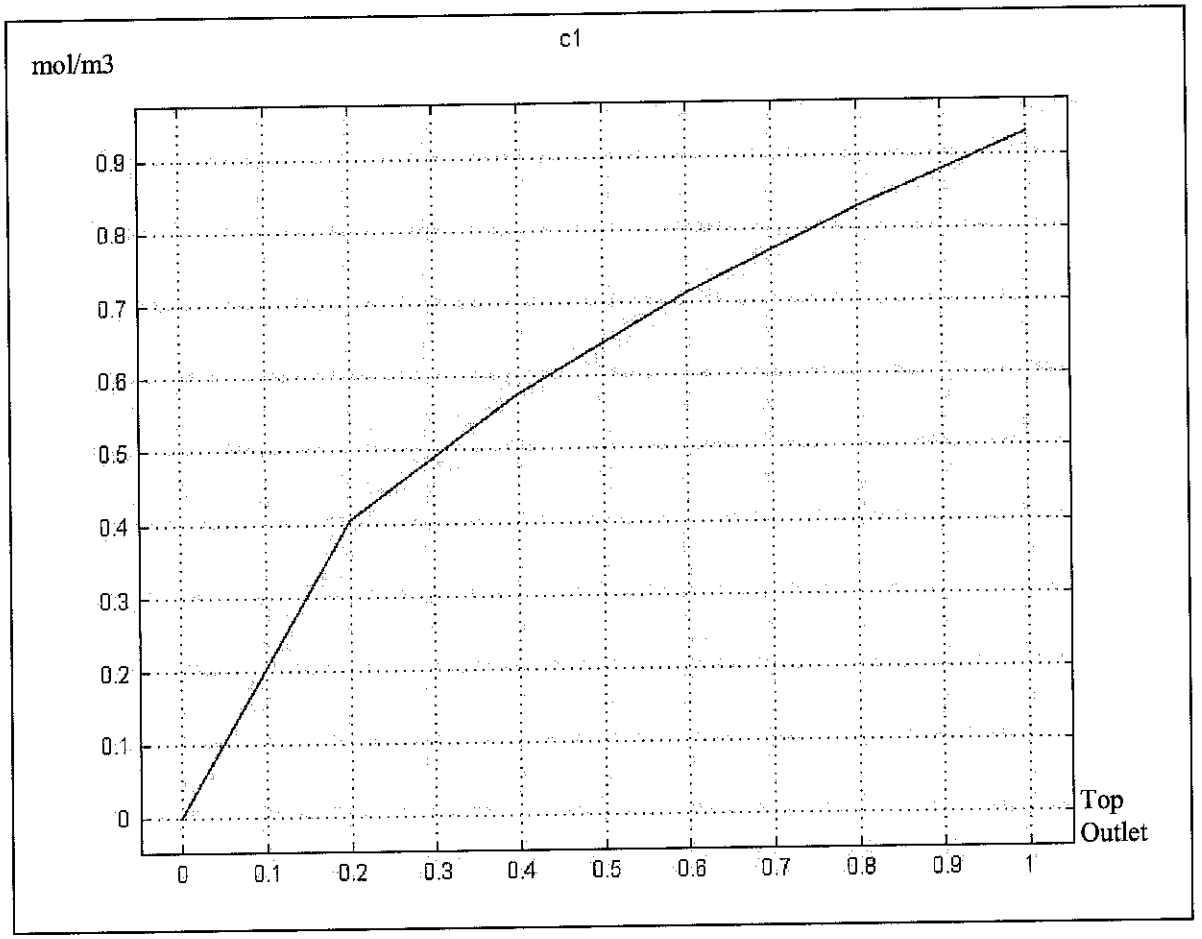

Figure 4.1.3c: Concentration profile of CO_2 absorbed at Concentration of CO_3^{2-} = 0.06 mol/m^3. (Run 7)

4.1.4 Run 7, Run 8 and Run 9 Results

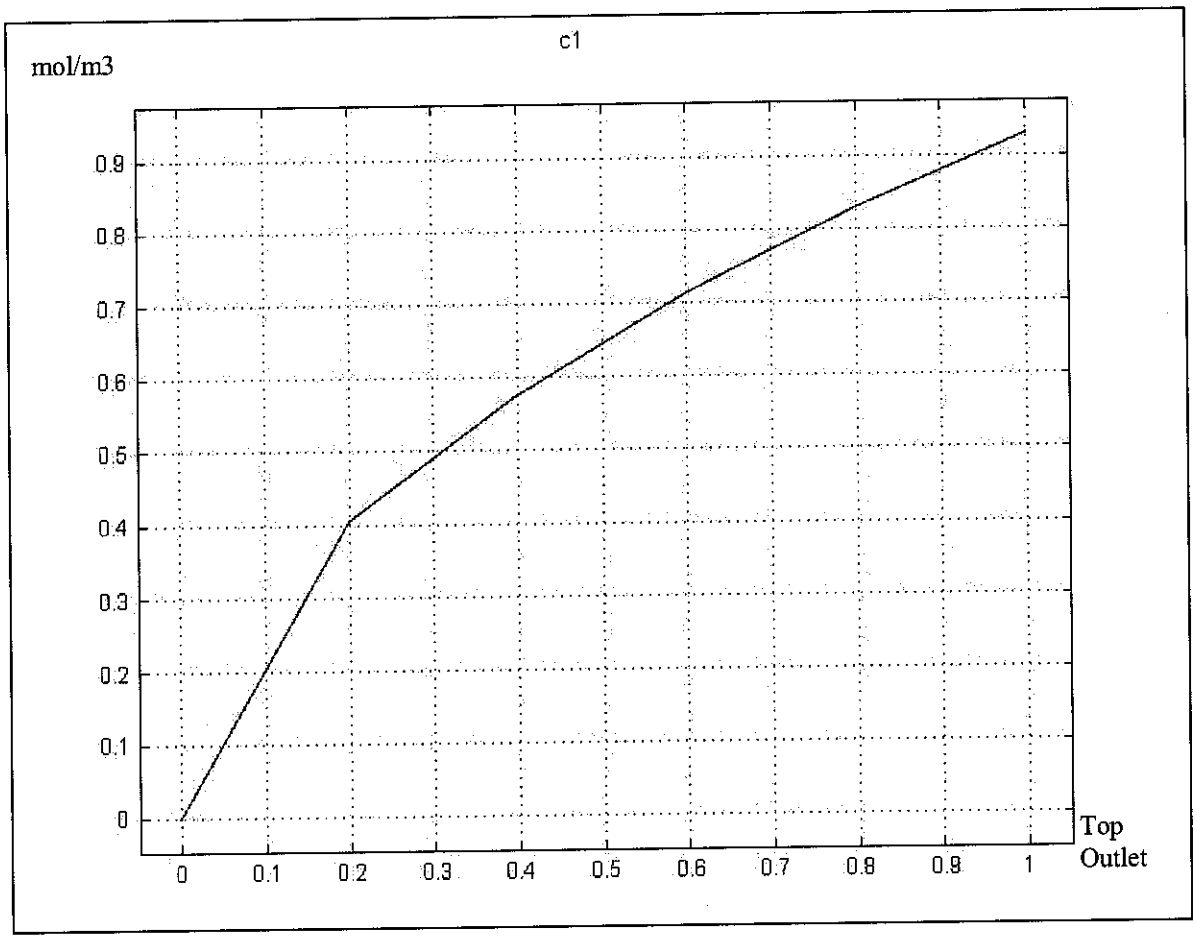

Figure 4.1.4a: Concentration profile of CO_2 absorbed at Concentration of DEA^- = 0.002mol/m^3. (Run 7)

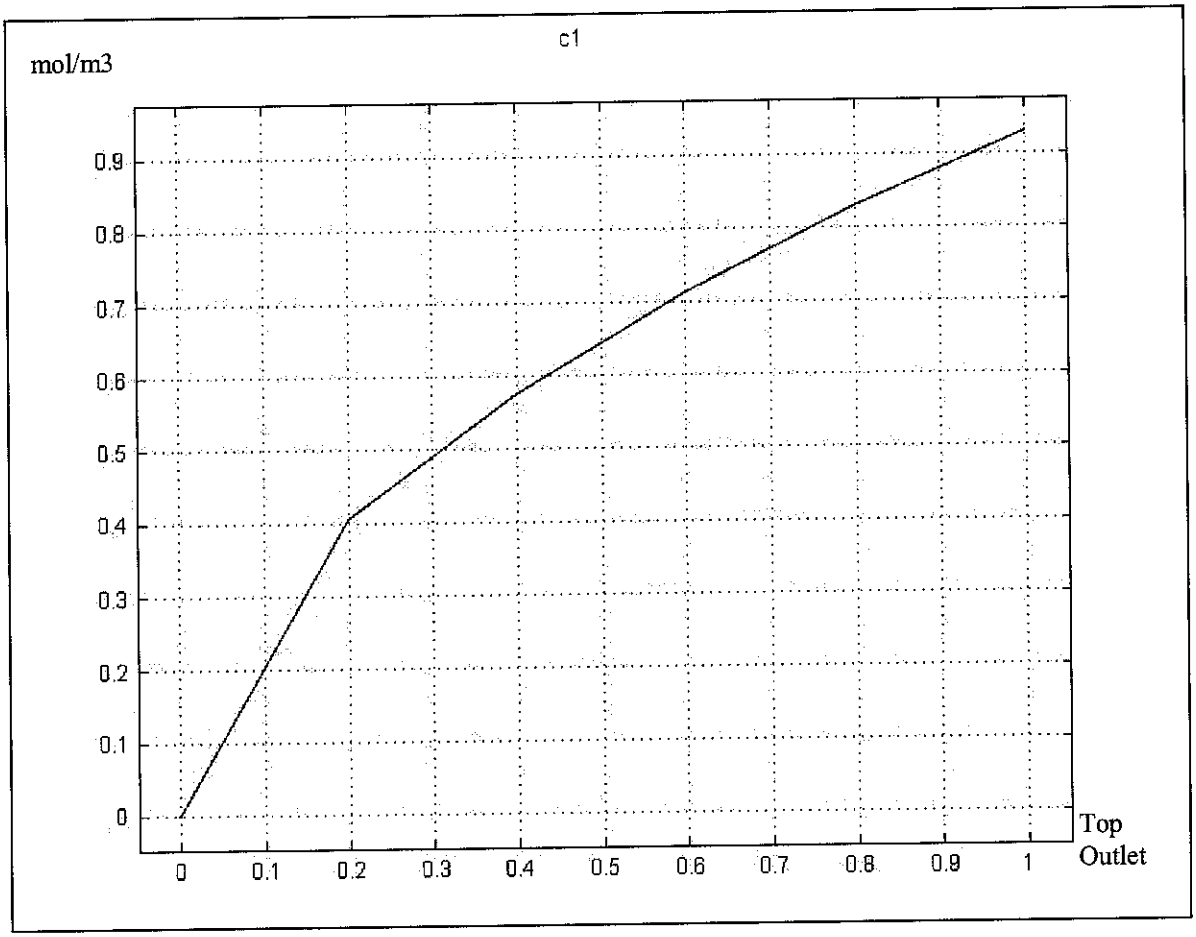

Figure 4.1.4b: Concentration profile of CO_2 absorbed at Concentration of DEA^- = 0.00001 mol/m^3. (Run 8)

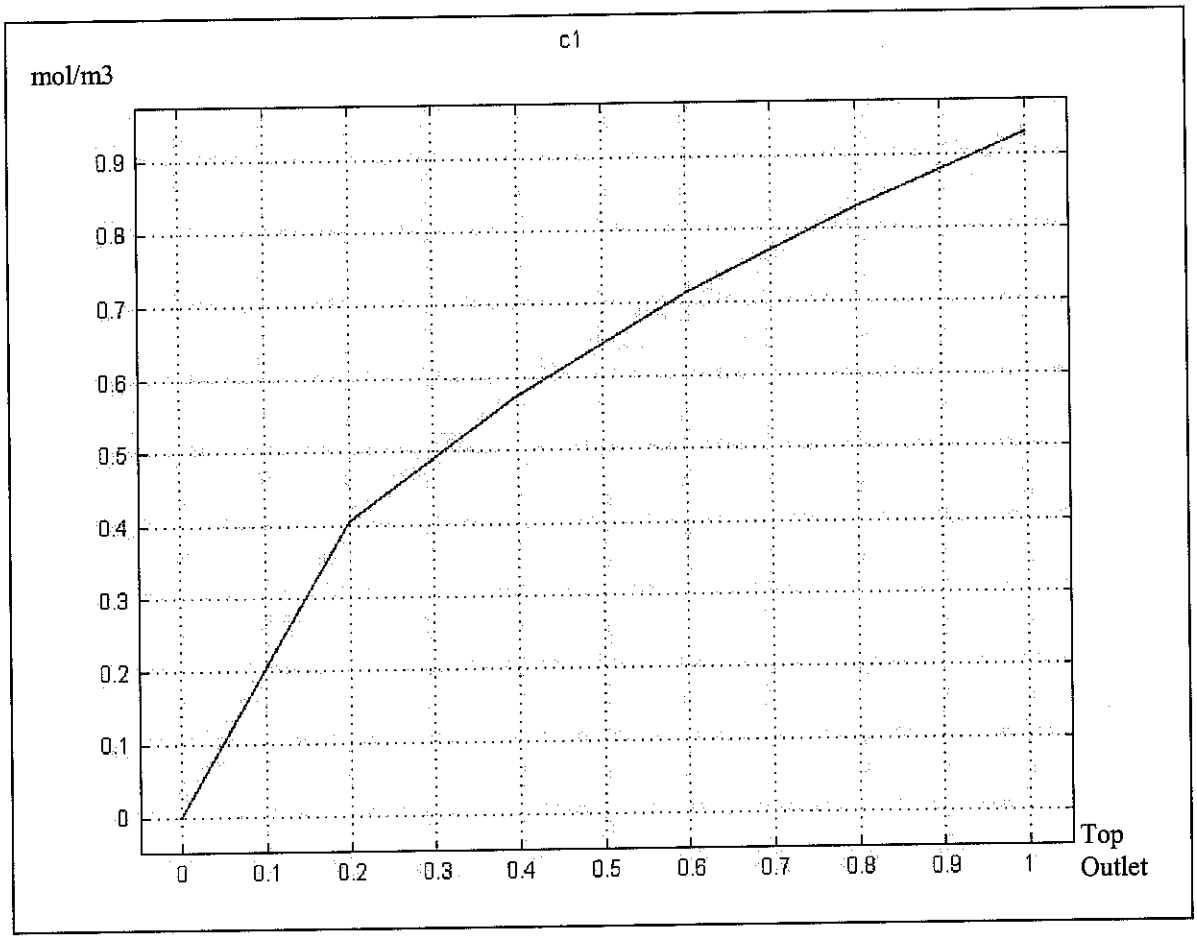

Figure 4.1.4c: Concentration profile of CO_2 absorbed at Concentration of DEA^- = 0.001mol/m^3. (Run 9)

EVIER

Chemical Engineering Science 59 (2004) 3619–3630

Chemical Engineering Science

www.elsevier.com/locate/ces

ırbon dioxide absorption with aqueous potassium carbonate promoted by piperazine

J. Tim Cullinane, Gary T. Rochelle*

Department of Chemical Engineering, 1, University Station C0400, The University of Texas at Austin, Austin, TX 78712, USA

Received 5 August 2002; received in revised form 28 January 2004; accepted 31 March 2004

'act

ıny commercial processes for the removal of carbon dioxide from high-pressure gases use aqueous potassium carbonate systems oted by secondary amines. This paper presents thermodynamic and kinetic data for aqueous potassium carbonate promoted by azine. Research has been performed at typical absorber conditions for the removal of CO_2 from flue gas.
ɔerazine, used as an additive in 20–30 wt% potassium carbonate, was investigated in a wetted-wall column using a concentration 5 m at 40–80°C. The addition of 0.6 m piperazine to a 20 wt% potassium carbonate system decreases the CO_2 equilibrium partial ure by approximately 85% at intermediate CO_2 loading. The distribution of piperazine species in the solution was determined by proton .. Using the speciation data and relevant equilibrium constants, a model was developed to predict system speciation and equilibrium. e addition of 0.6 m piperazine to 20 wt% potassium carbonate increases the rate of CO_2 absorption by an order of magnitude at 60°C. ate of CO_2 absorption in the promoted solution compares favorably to that of 5.0 M MEA. The addition of 0.6 m piperazine to 20 wt% sium carbonate increases the heat of absorption from 3.7 to 10 kcal/mol. The capacity ranges from 0.4 to 0.8 mol-CO_2/kg-H_2O for $_2CO_3$ solutions, comparing favorably with other amines.

ords: Absorption; CO_2 removal; Gas treating; Kinetics; Phase equilibria; Separations

ıtroduction

ıe absorption of carbon dioxide with amine or potas- ı carbonate solvents has gained widespread acceptance the removal of CO_2 from natural gas and H_2. Pri- y and secondary amines react with CO_2 to form amine amates. Aqueous primary amine solutions, such as oethanolamine (MEA), have been shown to have fast tion rates (Astarita, 1961). While aqueous secondary ıes, such as diethanolamine (DEA), are common, their tion rates have been found to be somewhat slower than ıary amines. Numerous investigators have explored the bility and reaction rate of CO_2 in aqueous potassium onate (Benson et al., 1954, 1956; Tosh et al., 1959). se studies indicate that potassium carbonate has a low of regeneration, but its rate of reaction is slow com- d to amines.

Several researchers have shown that the blending of amines accelerates the absorption process (Bosch et al., 1989a; Bishnoi, 2000; Dang, 2001). Likewise, many have investigated amine/potassium carbonate blends with some success (Savage and Sartori, 1984; Tseng et al., 1988; Bosch et al., 1989b).

This work focuses on expanding the investigation of promoted potassium carbonate (K_2CO_3) using piperazine (PZ) as the amine. Previous research has indicated that PZ is an effective promoter in methyldiethanolamine (MDEA) and MEA solutions (Bishnoi, 2000; Dang, 2001). Piperazine has a cyclic diamine structure that may favor rapid formation of the carbamates. As a mild base, it may serve to catalyze proton extractions in the reaction mechanism. Also, the molecule can theoretically absorb two moles of CO_2 for every mole of amine. The promoted potassium carbonate is expected to retain its low energy of regeneration, and the reaction of carbonate in the bulk solution is expected to give the solution a high capacity.

This work demonstrates that PZ is an effective promoter in potassium carbonate. The heat of absorption of CO_2 is

Corresponding author. Tel.: +1-512-471-7230; fax: +1-512-7824.
E-mail address: rochelle@che.utexas.edu (G.T. Rochelle).

-2509/$ - see front matter
0.1016/j.ces.2004.03.029

dependent on the relative concentrations of amines ıtassium carbonate. NMR indicates that PZ speciation, erefore loading, has a significant effect on absorption Equilibrium and rate modeling demonstrates the strong dence of capacity and the apparent rate constant of PZ tassium concentration. Experiments suggest that PZ mance is competitive with other amine systems.

ıterials and methods

: wetted-wall column, depicted in Fig. 1, was used as s–liquid contactor throughout the equilibrium and rate ments. The contactor is the same equipment used in ɔrk of Bishnoi (2000) and Dang (2001). The stainless vetted-wall, measuring 9.1 cm in height and 1.26 cm meter, is a tube extending from the liquid feed line ıe column housing. The chemical solution of interest ıped through the inside of the tube, overflows, and is / distributed across the outer surface of the tube. After tion at the base of the column, the fluid is pumped :o a liquid reservoir. Gas enters near the base of the n, counter-currently contacting the fluid as it flows up gas outlet.

: gas–liquid contact region is enclosed by a 2.54 cm ıick-walled glass tube, separating it from an insulat- yer of paraffin oil. The outermost region of the col- ıccommodates the circulating bath of paraffin oil in a cm OD thick-walled glass annulus.

: chemical solvent was contained in a 1.4 l reservoir ucted from a modified calorimetric bomb. A Cole– :r micropump pushes the solution from the reservoir ɡh a coil submerged in a heated circulator. After heat- ıe solution flows into the wetted-wall column. After

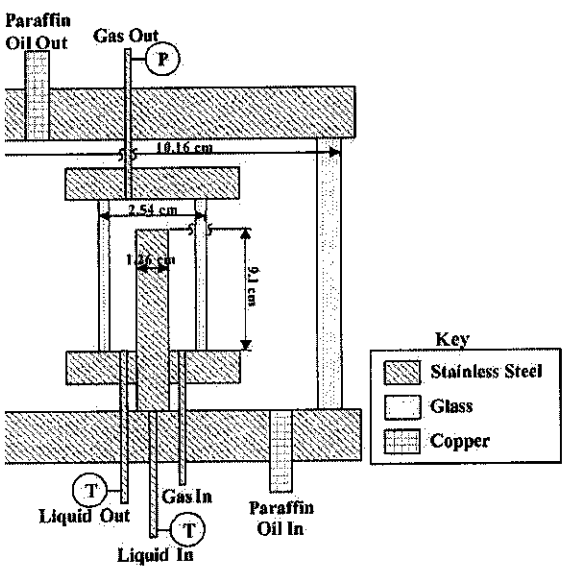

Fig. 1. Schematic of the wetted-wall column.

contacting the gas stream, the solvent returns to the reservoir, flowing through a rotameter for flowrate determination.

A 20 SLPM mass flow controller was used to meter nitrogen flow. The carbon dioxide flowrate was metered with a 1 SLPM mass flow controller. The metered gases were mixed prior to entering the wetted-wall column and were saturated with water in a calorimetric bomb heated in a water bath. After exiting the contactor, excess water was removed by passing the stream through a condenser. A drying column filled with magnesium perchlorate removed the remaining moisture. A carbon dioxide analyzer was used to measure the CO_2 concentration of the dry gas with infrared spectroscopy.

The inlet gas flowrate and the outlet gas flowrate provide the necessary information to calculate the flux of CO_2 into, or out of, the solvent. The partial pressure of carbon dioxide was varied, giving both absorption and desorption conditions. From this, an equilibrium partial pressure was interpolated.

Liquid samples, taken from the wetted-wall column at steady state conditions, were diluted and injected into a reaction vessel for analysis using an infrared, gas analyzer. The sample was reacted with 30 wt% phosphoric acid, stripping the CO_2 present. A calibration curve was obtained from a known CO_2 source (7 mM Na_2CO_3) and the concentration of CO_2 in the liquid samples was calculated. Measurements indicated that measured concentrations of CO_2 matched the nominal amount of CO_2 input into the solution; therefore, the nominal CO_2 concentration was used to define solution loading.

Proton spectra were obtained with a Varian INOVA 500 NMR to determine piperazine speciation in K_2CO_3. Characteristic peaks for piperazine, piperazine carbamate, and piperazine dicarbamate were previously determined by ^{13}C NMR and correlated to ^{1}H spectra for quantitative interpretation of peak areas (Bishnoi, 2000). In the samples, deuterated water (99.9% purity) was substituted for DI water.

Solutions were prepared with potassium carbonate, potassium bicarbonate or potassium hydroxide, and piperazine. The potassium carbonate, 99.6% pure, and the potassium bicarbonate, 99.9% pure, were purchased from Mallinckrodt. Potassium hydroxide from EM Science was > 85% pure. Anhydrous piperazine of greater than 99% purity was ordered from Aldrich Chemical Company. Solution CO_2 loading was varied using ratios of carbonate and bicarbonate or carbonate and hydroxide.

3. Modeling and data representation

3.1. Modeling equilibrium

A simple thermodynamic model was developed to predict the equilibrium and speciation in promoted potassium carbonate. This model was adapted from previous modeling work by Bishnoi (2000) and Dang (2001). Representation

; solution was accomplished using a stand-alone FOR-
N code, which includes the reactions shown below for
absorption in PZ promoted K_2CO_3.

$$g) \leftrightarrow CO_2(aq), \tag{1}$$

$$aq) + 2 \cdot H_2O \leftrightarrow HCO_3^- + H_3O^+, \tag{2}$$

$$_3^- + H_2O \leftrightarrow CO_3^{2-} + H_3O^+, \tag{3}$$

$$_2O \leftrightarrow H_3O^+ + OH^-, \tag{4}$$

$$H_2O + CO_2(aq) \leftrightarrow PZCOO^- + H_3O^+, \tag{5}$$

$$^+ + H_2O \leftrightarrow PZ + H_3O^+, \tag{6}$$

$$)O^- + H_2O + CO_2(aq) \leftrightarrow PZ(COO^-)_2 + H_3O^+, \tag{7}$$

$$ZCOO^- + H_2O \leftrightarrow PZCOO^- + H_3O^+. \tag{8}$$

e equilibrium constants for the reactions are shown in
; 1. These reactions, along with total mole balances
ı charge balance, were used to arrive at an equilibrium
ion composition.

ınry's constant for CO_2 in an aqueous solution was
ıated using the method of Danckwerts (1970). This
od involves ion specific constants describing the solu-
· of CO_2 in high ionic strength solutions. For the pur-
; of this work, Henry's constant was calculated for the
$O_3/KHCO_3$ concentrations; PZ was assumed to have no
t on gas solubility.

lieu of using activity coefficients, equilibrium constants
adjusted to match experimental data with high potas-
concentrations. An un-promoted potassium carbonate
ion at 60°C was used as a starting point for the model
.djustments, notated as β, to the equilibrium constants
made such that the new equilibrium constants are rep-
ıted as

$$_3^- = \beta \cdot K_{HCO_3^-}, \tag{9}$$

$$_- = \beta^2 \cdot K_{CO_3^{2-}} \tag{10}$$

used in this context, represents an activity coefficient
defined by the given reaction. Using a least squares
:ssion of the model predictions, β was altered so that
nodel fits smoothed $P^*_{CO_2}$ data at 60°C as extrapolated
Tosh et al. (1959).

ır a 20 wt% K_2CO_3 solution, no adjustment was neces-
indicating that the ratio of adjustment factors, β^2: β as
in Eqs. (9) and (10), must equal approximately one.
model was also compared to the 30 wt% K_2CO_3 so-
n investigated by Tosh et al. (1959). The value of β,
is case, was found to be 0.31 demonstrating the large
idealities associated concentrated electrolyte solutions.

A similar procedure was followed to match data for the speciation of PZ in the solutions, with each equilibrium constant treated independently (Cullinane, 2002). For a 20 wt% K_2CO_3 solution containing 0.6 m PZ at 60°C, the equilibrium constants were adjusted by matching predictions to NMR speciation data so that

$$K'_{PZCOO^-} = 0.75 \cdot K_{PZCOO^-}, \tag{11}$$

$$K'_{PZ(COO^-)_2} = 0.70 \cdot K_{PZ(COO^-)_2}. \tag{12}$$

The constants regressed allowed relatively accurate VLE modeling for the conditions considered in this work.

3.2. Modeling diffusion with chemical reaction

In addition to the equilibrium model, a rate model has been developed to predict the flux of CO_2 into the solvent. Rigorous accounting of equilibrium and mass transfer effects has allowed the estimation of rate constants suitable for describing the observed absorption phenomena.

Mass transfer is an important consideration and must be considered in modeling absorption processes. For the modeling of the boundary layer of CO_2 absorption, Bishnoi (2000) found that the eddy diffusivity theory, shown in Eq. (13) with a pseudo-first order assumption in the reaction term, performed as well as the Higbie penetration theory and the surface renewal theory. With the advantage of being a time-independent equation, this theory was selected for use in modeling in this work. Further details concerning the solution to this equation can be found in Glasscock (1990).

$$\frac{\partial}{\partial x}\left[(D_{CO_2} + \varepsilon x^2)\frac{\partial[CO_2]}{\partial x}\right] - k_1[CO_2] = 0. \tag{13}$$

Bishnoi (2000) developed a rate model that integrates the ordinary differential equation for eddy diffusivity using multiple nodes across a dimensionless boundary layer. The solution is a function of gas film resistance, liquid film resistance of reactants and products, and bulk solution composition. The model requires an estimation of the diffusion coefficient of reactants and products, but accounts rigorously for gas phase resistance, equilibrium, and kinetics within the gas–liquid interface. The diffusion coefficient was assumed to be that of CO_2 in water and was calculated by the expression given in Versteeg and van Swaaij (1988).

$$D_{CO_2}(m^2/s) = 2.35 \times 10^{-6} \exp\left(\frac{-2119}{T(K)}\right). \tag{14}$$

The model predicts a flux by using a bulk gas phase partial pressure of CO_2 and the bulk solution composition as found by the equilibrium model. The model iteratively solves for an interface partial pressure until a continuous solution is obtained, satisfying the gas film and liquid film resistances. The absorption rates predicted by the model were compared to experimental data. With the use of a non-linear regression package, GREG (Caracotsios, 1986), rate constants were

1
rium equations in equilibrium model, mole fraction-based

Equilibrium Constant	$\ln K_i = A + B/T + C \ln T$			Source
	A	B	C	
$K_{HCO_3^-} = \frac{x_{HCO_3^-} \cdot x_{H_3O^+}}{x_{CO_2} \cdot x_{H_2O}^2}$	231.4	−12092	−36.78	Edwards et al. (1978), Posey (1996)
$K_{CO_3^{2-}} = \frac{x_{H_3O^+} \cdot x_{CO_3^{2-}}}{x_{HCO_3^-} \cdot x_{H_2O}}$	216.0	−12432	−35.48	Edwards et al. (1978), Posey (1996)
$K_w = \frac{x_{H_3O^+} \cdot x_{OH^-}}{x_{H_2O}^2}$	132.9	−13446	−22.48	Edwards et al. (1978), Posey (1996)
$K_{PZCOO^-} = \frac{x_{PZCOO^-} \cdot x_{H_3O^+}}{x_{PZ} \cdot x_{CO_2} \cdot x_{H_2O}}$	−29.31	5615	0.0	Bishnoi (2000)
$K_{PZH^+} = \frac{x_{PZ} \cdot x_{H_3O^+}}{x_{PZH^+} \cdot x_{H_2O}}$	−11.91	−4351	0.0	Pagano et al. (1961)
$K_{PZ(COO^-)_2} = \frac{x_{PZ(COO^-)_2} \cdot x_{H_3O^+}}{x_{PZCOO^-} \cdot x_{CO_2} \cdot x_{H_2O}}$	−30.78	5615	0.0	Bishnoi (2000)
$K_{H^+PZCOO^-} = \frac{x_{PZCOO^-} \cdot x_{H_3O^+}}{x_{H^+PZCOO^-} \cdot x_{H_2O}}$	−8.21	−5286	0.0	Bishnoi (2000)

ted so that a minimum in the least squares error was ned.

addition to the rigorous rate model, the data was ana- with the common pseudo-first order assumption. Many , amine reactions can be considered first order in CO_2 ntration and first order in amine concentration. Under al conditions, the amine is at a nearly constant concen- n across the boundary layer and the reaction rate can presented by a pseudo-first order rate constant, k_1, and oncentration of CO_2 as in Eq. (13). Under these con- is, the solution for the flux is

$$= \frac{\sqrt{D_{CO_2} k_{Am} [Am]_b}}{H_{CO_2}} (P_{CO_2,i} - P^*_{CO_2}), \tag{15}$$

e the pseudo-first order rate constant is replaced by a constant, k_{Am}, and the concentration of the amine in the solution, $[Am]_b$. $P_{CO_2,i}$ and $P^*_{CO_2}$ represent the partial ure of CO_2 at the interface and the equilibrium partial ure of CO_2 in the bulk solution, respectively.

is important to recognize that the liquid phase driving must necessarily be small to satisfy the assumption gligible depletion of amine across the boundary layer. validity of this assumption was tested by comparing the ntaneous flux to the actual, measured flux. The instan- us flux can be calculated by

$$= k_{l,\text{prod}}([CO_2]^*_{T,i} - [CO_2]_{T,b}), \tag{16}$$

e $[CO_2]^*_{T,i}$ is the concentration of all CO_2 species in ibrium with the gas phase at the interface, $[CO_2]_{T,b}$ is otal CO_2 concentration in the bulk solution, and $k_{l,\text{prod}}$ e liquid phase transfer coefficient of the products of reaction. This was estimated as

$$k_{l,\text{prod}} = k_l \sqrt{\frac{D_{\text{prod}}}{D_{CO_2}}}, \tag{17}$$

where k_l is the liquid phase transfer coefficient of CO_2. D_{prod} and D_{CO_2} are the diffusion coefficients of products and CO_2, respectively, whose ratio was estimated as 0.5.

The actual flux is defined similarly; however, the concentration of CO_2 species at the interface, $[CO_2]_{T,i}$, is not in equilibrium with the gas. In this case, flux is represented by

$$N_{\text{act}} = k_{l,\text{prod}}([CO_2]_{T,i} - [CO_2]_{T,b}). \tag{18}$$

A ratio of actual and instantaneous flux, Eq. (19), gives an approach to instantaneous behavior. A small fraction indicates the pseudo-first order approximation is valid.

$$\frac{N_{\text{act}}}{N_{\text{inst}}} = \frac{[CO_2]_{T,i} - [CO_2]_{T,b}}{[CO_2]^*_{T,i} - [CO_2]_{T,b}}. \tag{19}$$

This analysis was performed on the data in this work to show that most of the data can be represented as pseudo-first order. This is only necessary for simplified representations of the data, not for the rigorous rate model predictions.

3.3. Reaction kinetics

In addition to the equilibria defined, modeling the absorption rate requires defining reaction rates important to the absorption mechanism. In this work, Eqs. (2), (5), and (7) were considered with reversible rate expressions. The remaining equations were considered to be in equilibrium.

The reaction mechanism of CO_2 absorption into water consists of the conversion of carbonate to bicarbonate (Eq. (2)). The controlling mechanism, however, is generally

as a reaction of CO_2 with a hydroxyl ion to give a ›onate ion.

$$+ OH^- \leftrightarrow HCO_3^-. \tag{20}$$

ıte is well defined and can be predicted using a second rate constant that is proportional to the hydroxyl con- ıtion and corrected for ionic strength (Astarita et al.,).

$$_{OH} = 13.635 - 2895/T + 0.08I. \tag{21}$$

: reversible rate defined in terms of concentrations and :fined equilibrium constants is

$$_{OH^-}\left([OH^-][CO_2] - \frac{K_{HCO_3^-}}{K_w}[HCO_3^-]\right). \tag{22}$$

rate is considerably slower than the reaction of CO_2 amines and plays only a minor role in defining CO_2 ption in amine-based solvents.

: accepted mechanism of amines reacting with CO_2, vitterion mechanism, was proposed by Caplow (1968). s mechanism, the CO_2 and the amine form a zwitterion nediate (Eq. (23)). Following formation, the interme- can be deprotonated by a base, such as the free amine (24)) or water.

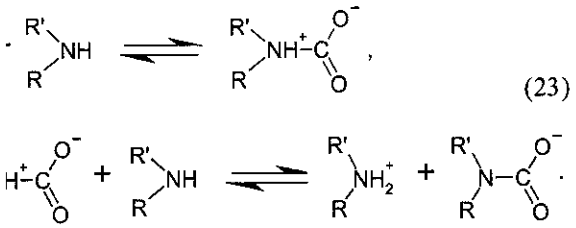

(23)

(24)

th this mechanism, the kinetic expression, as given by kwerts (1970), can be expressed as

$$\frac{k_f[CO_2][Am]}{+ k_r/\sum k_b[B]}. \tag{25}$$

, when the formation of the intermediate is the rate olling step, the contribution of the bases, $\Sigma k_b[B]$, is and the denominator reduces to a value of one. When ›tonation of the intermediate is rate controlling, $\Sigma k_b[B]$ all so that the denominator must be considered.

this work, the forward rate of PZ reacting with CO_2 was sented as a zwitterion mechanism in which hydroxide vater are the acting bases for proton extraction. This to the following expansion of Eq. (25):

$$\frac{k_f[CO_2][Am]}{+ [k_r/k_{b,OH^-}[OH^-] + k_{b,H_2O}]}, \tag{26}$$

: k_{b,OH^-} represents the extraction of protons from PZ by and k_{b,H_2O} represent a pseudo-zero order rate constant iated with the extraction of protons by water from PZ. expression can be further simplified by assuming the 1 : denominator is negligible compared to the contribution : bases and by combining the rate constants. With this simplification, the reversible rate for Eq. (5) can be written as

$$r = (k_{PZ} + k_{PZ-OH^-}[OH^-]) \times \left([PZ][CO_2] - \frac{K_W}{K_{PZCOO^-}}\frac{[PZCOO^-]}{[OH^-]}\right), \tag{27}$$

where k_{PZ} is the combination of k_{b,H_2O}, k_f, and k_r and k_{PZ-OH} is defined similarly.

Likewise, for Eq. (7) it is found that the reversible rate is

$$r = k_{PZCOO^-}\left([PZCOO^-][CO_2] - \frac{K_W}{K_{PZ(COO^-)_2}}\frac{[PZ(COO^-)_2]}{[OH^-]}\right). \tag{28}$$

The concentration of hydroxide is negligible at any condition where $PZCOO^-$ is significant and is, therefore, not considered as an acting base in this reaction.

3.4. Representation of experimental data

The flux of CO_2 into or out of the solution can be characterized by mass transfer coefficients such as the overall gas transfer coefficient.

$$N_{CO_2} = K_G(P_{CO_2,b} - P^*_{CO_2}). \tag{29}$$

Data was taken at various bulk partial pressures such that the equilibrium partial pressure, $P^*_{CO_2}$, could be found by considering points close to equilibrium and interpolating to a flux of 0.0. The overall mass transfer coefficient, K_G, is calculated as the slope of the flux versus the log mean pressure, ΔP_{lm}. The ΔP_{lm} is defined as a log mean difference in bulk gas partial pressures of CO_2 across the wetted-wall column.

$$\Delta P_{lm} = \frac{P_{CO_2,in} - P_{CO_2,out}}{\ln(P_{CO_2,in}/P_{CO_2,out})}. \tag{30}$$

A demonstration of this procedure is shown in Fig. 2.

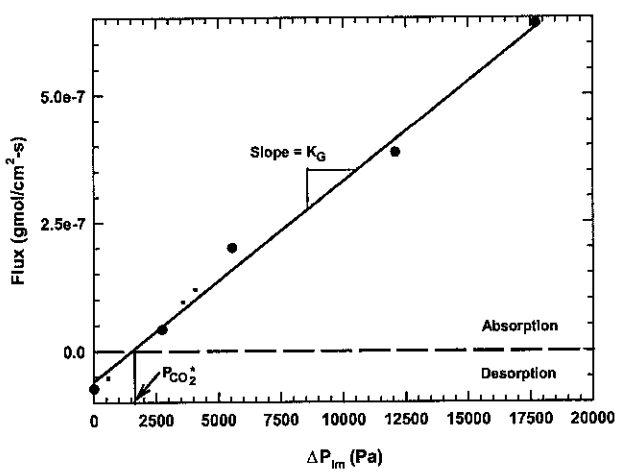

Fig. 2. Determination of $P^*_{CO_2}$ and K_G for 3.6 m K^+/0.6 m PZ at 40°C and $\alpha = 0.221$.

: gas phase mass transfer coefficient, k_g, for the l-wall column was calculated using a correlation nined by Pacheco (1998).

$$1.075\left(ReSc\frac{d}{h}\right)^{0.85}, \tag{31}$$

: Re is the Reynolds number, Sc is the Schmidt number, ıe hydraulic diameter of the column, and h is the height column. The Sherwood number, Sh, yields k_g from

$$\frac{RTk_gh}{D_{CO_2}}, \tag{32}$$

: R is the gas constant, T is temperature, and D_{CO_2} is ffusion coefficient of CO_2.

: liquid film resistance can be written as

$$= k_g'(P_{CO_2,i} - P^*_{CO_2}), \tag{33}$$

: k_g' is a normalized flux, a mass transfer coefficient for ırtial pressure driving force across the liquid film. The ılized flux was calculated from the following expres-

$$\left(\frac{1}{K_G} - \frac{1}{k_g}\right)^{-1}. \tag{34}$$

that the value of k_g' as calculated from experimental loes not require any pseudo-first order assumption.

esults and discussion

Speciation

e relative concentration of each piperazine species was nined by proton NMR (Cullinane, 2002) and is given function of composition, loading, and temperature ble 2. Note that NMR does not distinguish between otonated and protonated forms of the same species. ıerature has a minimal effect on the speciation; how- free piperazine concentration generally increases as ɜrature increases (Fig. 3).

ading has a significant effect on speciation as shown in l. In this sample, piperazine carbamate and piperazine ɔamate do not exist at low loading. There is a maxi- fraction of piperazine carbamate at a loading near 0.0. gh loading, piperazine dicarbamate becomes an im- nt species, but a significant concentration of the reac- ıpecies piperazine carbamate remains. Loading trends ıer temperatures are comparable (Fig. 5).

e continuous lines in Figs. 3–5 are predictions of the ibrium model. Throughout the range of loading, the l performs well. There is a slight discrepancy at high ng where the model over-predicts the conversion of azine to its carbamate form and the conversion of carba- to dicarbamate. Model accuracy diminishes as temper- moves away from 60°C, the temperature of the equi- m constant regressions, indicating that ionic strength affect the temperature dependence of piperazine equi- m constants.

Table 2
Integrated NMR peaks as percentage of piperazine species

$[K^+]$ (m)	[PZ] (m)	Loading[a]	T (K)	$PZ + PZH^+$ (%)	$PZCOO^- + H^+PZCOO^-$ (%)	$PZ(COO^-)_2$ (%)
3.6	0.6	−0.347	303	99.3	0.7	0.0
			313	99.3	0.7	0.0
			333	99.5	0.6	0.0
		−0.229	303	78.2	21.8	0.0
			313	79.0	21.0	0.0
			333	78.0	22.0	0.0
		−0.032	303	18.4	47.3	34.3
			313	19.5	48.6	31.9
			333	22.7	49.3	28.0
		0.222	303	8.5	41.3	50.3
			333[b]	12.6	44.0	43.4
6.2	0.6	−0.035	313	19.7	49.2	31.1
			333	22.5	49.0	28.5
			353	32.5	39.1	28.4
		0.278	313	5.7	32.7	61.6

[a]mol $CO_{2,TOT}$/(mol PZ + mol K_2) − 1.
[b]Manual graphical integration in lieu of numerical integration.

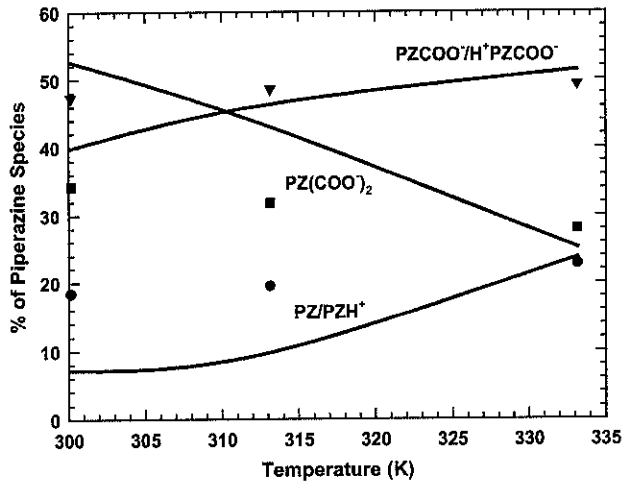

Fig. 3. Piperazine speciation in 3.6 m K^+/0.6 m PZ at $\alpha = -0.032$, points: NMR data, lines: model predictions.

4.2. Equilibrium

Fig. 6 shows the effects of PZ addition to potassium carbonate on CO_2 solubility. As shown by the continuous lines, the simple VLE model accurately predicts the equilibrium partial pressure in a solution of both promoted and un-promoted potassium carbonate. The less satisfactory fit at low loading suggests that the selected relationship for the adjustment factors does not hold at low loading conditions. A summary of all equilibrium data collected in the wetted-wall column is presented in Table 3.

The calculated solvent capacity of potassium carbonate solutions compares favorably to amine solvents as shown in

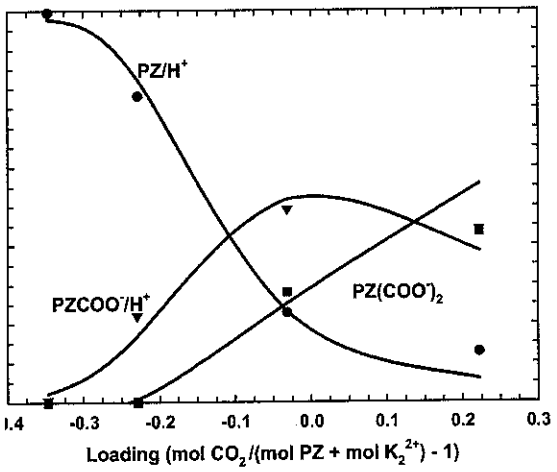

Piperazine speciation in 3.6 m K^+/0.6 m PZ at 60°C, points: ata, lines: model predictions.

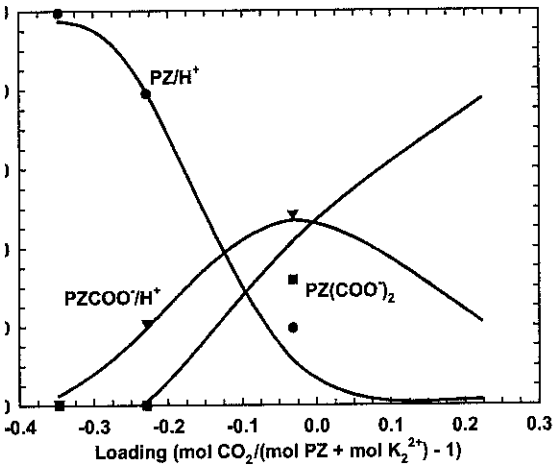

Piperazine speciation of 3.6 m K^+/0.6 m PZ at 40°C, points: ata, lines: model predictions.

4. The addition of 0.6 m PZ to 20 wt% K_2CO_3 yields ible changes in capacity. An increase in potassium ntration produces a large increase in solvent capacity, sting further increases would make the capacity equiv- o or greater than that of MEA.

heat of absorption of CO_2 was calculated from the rature dependence of the CO_2 solubility (Fig. 7). ddition of 0.6 m PZ to 20 wt% potassium carbonate ses the heat of absorption from 3.7 kcal/mol (Tosh 1959) to around 10 kcal/mol. With a comparable g and PZ concentration, more potassium carbonate to decrease the heat of absorption only slightly, ting that the amine is largely responsible for the re- with CO_2. A decrease in loading results in a marked se in the heat of absorption, most likely due to a nce in heats of absorption of piperazine and of piper- carbamate. These results also suggest that promoted

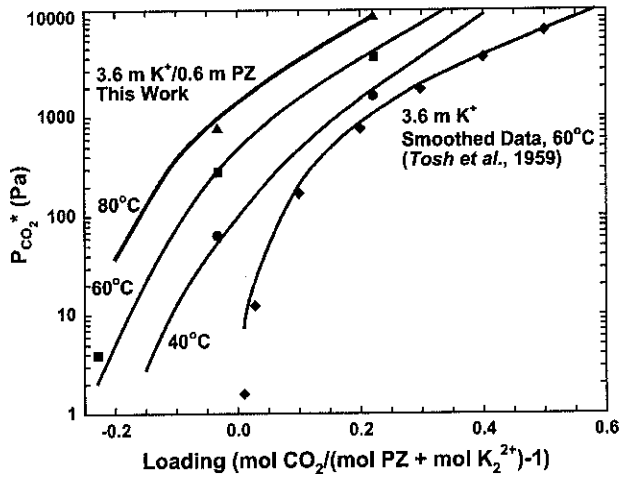

Fig. 6. CO_2 Equilibrium in promoted and un-promoted K_2CO_3, points: experimental data, lines: model predictions with $\beta = 1.0$.

potassium carbonate solutions would possess a lower heat of absorption than comparable amine systems.

4.3. Absorption rates

Table 3 and Figs. 8 and 9 summarize the normalized flux of CO_2 absorption as measured in the wetted-wall column. The addition of 0.6 m PZ to 3.6 m potassium yields a dramatic change in the rate of CO_2 absorption, increasing the normalized flux by a factor of ten at 60°C. The rate behavior of this solvent approaches that of 7 m MEA at both 40°C and 60°C. Increasing the potassium concentration to 4.8 m does little to affect the absorption rate. At a rich loading, both promoted K_2CO_3 solutions compare favorably with an MDEA/piperazine blend investigated by Bishnoi (2000). At a constant CO_2 vapor pressure, increasing the temperature from 40°C to 80°C increases the rate of CO_2 absorption by a factor of two (Fig. 9). In this temperature range, a reduction in gas solubility is countered by an increase in sorption kinetics.

The rate data of PZ-promoted K_2CO_3 is compared to data on two other promoters used in K_2CO_3 solutions, diethanolamine (DEA) and an unspecified hindered amine investigated by Sartori and Savage (1983), in Fig. 10. For this comparison, CO_2 loading was represented as conversion of CO_3^{2-} to HCO_3^- and Henry's constant was estimated accounting only for the K_2CO_3 in solution. While each promoter improves the rates over un-promoted K_2CO_3 to some degree, piperazine at 60°C gives the best improvement. From knowledge of the rate dependence on temperature, the other promoters, DEA and the hindered amine at 90°C, would compare even less favorably to piperazine at 90°C. This behavior can be partially attributed to improved rate behavior and partially to "salting out" of CO_2 at high temperatures and high ionic strengths.

Table 3
Summary of experimental results from the wetted-wall column, gas flow: 4–7 LPM, P_{CO_2}: 0–25,000 Pa, liquid flow: 2.5–3.5 cm^3/s, contact area: 38 cm^2

T (°C)	$[K^+]$ (m)	[PZ] (m)	Nominal loading[a]	$P^*_{CO_2}$ [b] (Pa) (WWC)	$P^*_{CO_2}$ (Pa) (Model)	Avg. $k_g \times 10^{10}$ [c] (gmol/Pa cm^2 s)	Avg. k_l^{oc} k_l^{oc} (cm/s)	$k'_g \cdot 10^{10}$ [d,e] (gmol/Pa cm^2 s)	Driving force[f] (Pa) Max.	Driving force[f] (Pa) Min.	$\frac{N_{act}}{N_{inst}}$ [g]
60	3.6	0.0	0.176	515 ± 50	728	2.02	0.012	0.11 ± 0.01	170	−440	0.00
			0.551	10369 ± 4990	10942	2.83	0.012	0.06 ± 0.01	14000	−7070	0.03
60	3.6	0.6	−0.347	< 1 ± 5	0	2.30	0.012	4.41 ± < 0.001	310	30	0.01
			−0.229	3 ± 1	2	2.18	0.013	2.47 ± < 0.001	160	18	0.01
			−0.032	279 ± 30	305	1.75	0.013	1.81 ± 0.08	270	−270	0.05
			0.222	3539 ± 1300	4784	3.00	0.012	0.48 ± 0.07	15310	−3510	0.21*
40	3.6	0.6	−0.033	64 ± 8	56	1.95	0.009	1.32 ± 0.18	390	−62	0.01
			0.221	1635 ± 340	1951	3.01	0.009	0.45 ± 0.03	16090	−1620	0.19*
80	3.6	0.6	−0.033	756 ± 50	1007	2.66	0.016	4.24 ± 0.39	3830	−230	0.24*
			0.221	10197 ± 80	10724	3.11	0.017	0.76 ± 0.03	7740	−6770	0.12
60	4.8	0.6	0.290	6212 ± 1070	6526	2.95	0.011	0.49 ± 0.03	14470	−6130	0.18*
40	4.8	0.6	0.290	2453 ± N/A	2978	3.08	0.008	0.26 ± 0.03	17650	390	0.11
80	4.8	0.6	0.290	14161 ± 4890	13533	3.20	0.015	0.52 ± 0.06	8650	−10560	0.16*
60	6.2	1.2	0.205	6014 ± 610	3805	2.75	0.010	0.55 ± 0.04	14270	−2420	0.22*

[a] mol-CO_2/(mol-PZ + mol-K_2) − 1.
[b] Found by interpolating to Flux = 0.
[c] Calculated as an average of individual data points taken from WWC.
[d] Calculated from slope of flux versus (P-P^*) for several data points.
[e] $k'_g = N_{CO_2}/(P_{CO_2,i} - P^*_{CO_2})$.
[f] Highest ($P_{CO_2,b} - P^*_{CO_2}$) in experiment.
[g] Actual flux/calculated instantaneous flux.
* Indicates a significant approach to instantaneous behavior.

' comparison of K_2CO_3 and amine solvents, lean: 0.01 atm CO_2, rich: 0.1 atm CO_2, 33% approach to equilibrium, 60°C

	3.6 m K^+	3.6 m K^+/0.6 m PZ	6.2 m K^+	7 m MEA	1.2 m PZ/8.5 m MDEA	10 m AMP
lg.[a] (m)	2.0	2.3	3.4	9.4	9.1	11.1
/ (m)	0.41	0.50	0.73	0.81	0.78	1.75

ing here is defined as mol CO_2/kg H_2O.

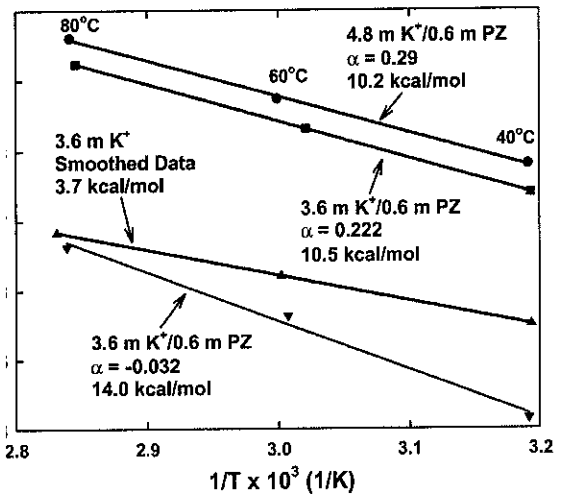

CO_2 heat of absorption in K_2CO_3/PZ, points: WWC data, lines: ression.

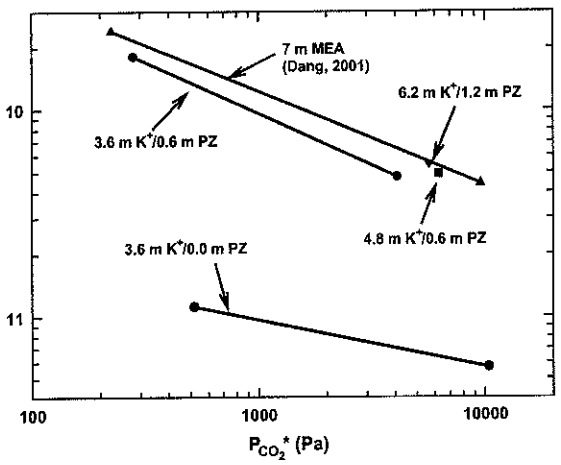

. CO_2 absorption rates in K_2CO_3 and MEA solutions at 60°C.

rate model was able to successfully predict values (by using regressed rate constants and temperature dences. As previously mentioned, GREG was used ve at rate constants suitable for Eqs. (27) and (28). esults of the regressions, including values obtained shnoi (2000) for aqueous piperazine, are shown in 5.

erazine and piperazine carbamate rate constants used model were of the form shown in Eq. (35) to account

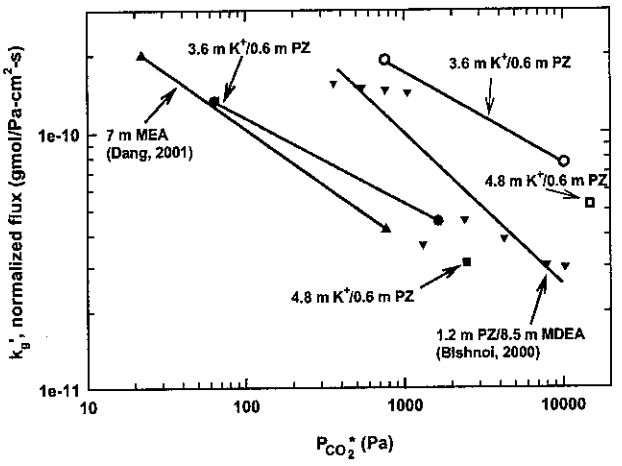

Fig. 9. CO_2 absorption rates in various solvents, closed points: 40°C, open points: 80°C.

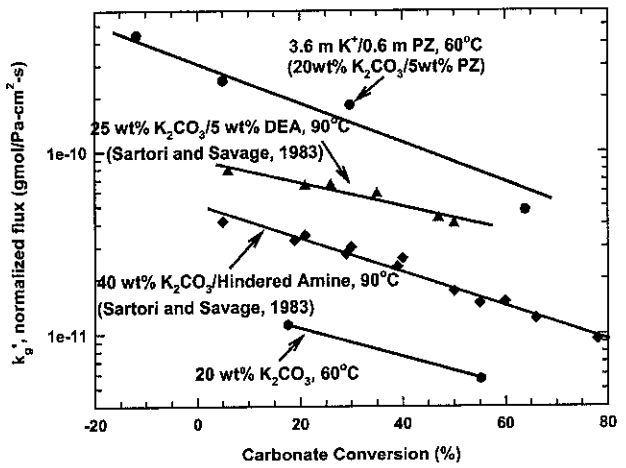

Fig. 10. Comparison of promoted K_2CO_3 solutions.

for temperature dependence. The PZ-hydroxide rate constant neglects temperature dependence, or $\Delta H_a = 0$.

$$k_i = k_i^{\circ} \exp\left[-\frac{\Delta H_a}{R}\left(\frac{1}{T} - \frac{1}{298.15\ \mathrm{K}}\right)\right]. \tag{35}$$

It should be recognized that, while the k_g' reported is valid for all data, rigorous modeling as performed in this work is required to account for instantaneous behavior and obtain an actual rate constant. Several solutions in Table 3 are noted with an asterisk, indicating that the effect of instantaneous rate is becoming significant. These solutions are typically at

; rate constants regressed from various rate equations, $\Delta H_a = 3.36e4$ kJ/mol for piperazine and piperazine carbamate (Bishnoi, 2000)

	Piperazine-hydroxide $k^o_{PZ\text{-}OH}$ ($m^6/kmol^2$ s)	Piperazine k^o_{PZ} (m^3/kmol s)	Piperazine carbamate $k^o_{PZCOO^-}$ (m^3/kmol s)
i (2000)	0.0[a]	5.38e4	4.70e4
ork (Fig. 11)	0.0[a]	1.29e6	1.93e4
ork (Fig. 12)	2.69e6[b]	2.85e5	4.70e4[a]

regressed.
$I_a = 0$ kJ/mol.

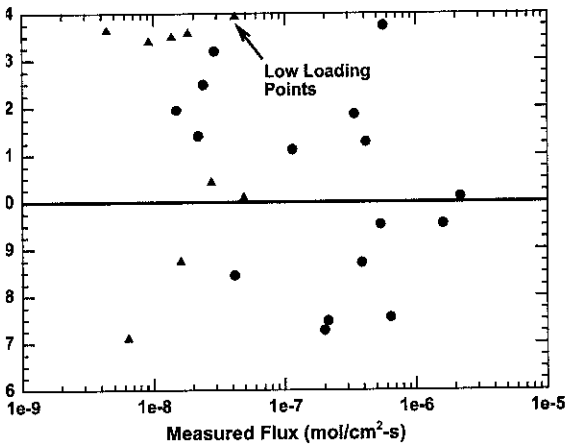

1. Parity plot of promoted K_2CO_3 fluxes with two regressed rate nts: $k^o_{PZ} = 1.29e6$ M^{-1} s^{-1} and $k^o_{PZCOO^-} = 1.93e4$ M^{-1} s^{-1}.

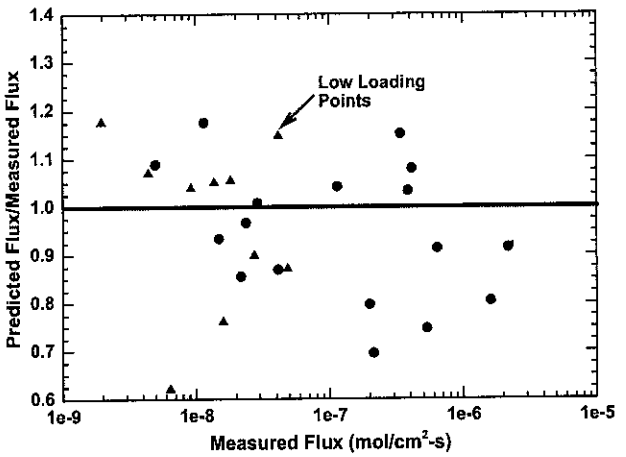

Fig. 12. Parity plot of promoted K_2CO_3 fluxes with three regressed rate constants: $k_{PZ-OH^-} = 2.69e6$ M^{-2} s^{-1}, $k^o_{PZ} = 2.85e5$ M^{-1} s^{-1}, and $k^o_{PZCOO^-} = 4.70e4$ M^{-1} s^{-1}.

loading or high temperature. The approach to instan- us rate is a "worst case" estimate for amine depletion s the boundary layer and represents the highest frac- 'or a data set. Most of the data, however, could be well sented by a pseudo-first order approximation. In this the kinetics could be found from

$$\frac{\sqrt{D_{CO_2} k_{Am} [Am]_b}}{H_{CO_2}} \tag{36}$$

ving the form of Eq. (15).

o regressions of the data were performed without and the PZ-hydroxide rate constant (Cullinane, 2002). The ting fits of data for 3.6 m K^+/0.6 m PZ are shown in 11 and 12. Note that without the PZ-hydroxide rate ant, seemingly unreasonable changes in the rate con- s occur and an unsatisfactory fit of the data results, par- rly at low loadings. By including a term prevalent only w loadings, the PZ-hydroxide rate constant, the fit is oved and more reasonable rate constants are obtained. ing the low loading interaction term, the PZ rate con- is increased by a factor of five from its value in water as ted in Bishnoi (2000). The rate constant for piperazine mate gives satisfactory results when its value in 8.5 m A is used (Bishnoi, 2000). Previous research suggests ccelerated rate behavior is a result of a catalytic ef- f carbonate or of increased ionic strength. Laddha and kwerts (1982) compared effects of K_2CO_3 and K_2SO_4 on MEA and DEA and found that potassium carbonate significantly increases the kinetics of DEA above ionic strength contributions from potassium sulfate addition, suggesting a catalytic effect of the carbonate. The kinetics of MEA are affected equivalently by K_2CO_3 and K_2SO_4. Sartori and Savage (1983) and Tseng et al. (1988) also report accelerated rate behavior of DEA/carbonate solutions. Pohorecki et al. (1988) found, however, that the rate constant of ethylaminoethanol, another secondary amine, is a function of ionic strength, not carbonate concentration. The current data on PZ/K_2CO_3 does not support attributing the increased kinetics specifically to ionic strength or to carbonate concentration.

The PZ-hydroxide term at a high concentration of hydroxide, 0.45 M, in 3.6 m K^+ gives an apparent rate constant 22 times faster than in water. This may indicate that the proton extraction, rather than the formation of the zwitterion intermediate, is the rate-limiting step. With large amounts of the strong base hydroxide, it would be expected that this term would be required at low loading. If the proton extraction is rate-limiting even at the low loading conditions (i.e. more base), it is implied that it should be rate-limiting at high loading conditions where there is less base for the catalysis effect.

The simple rate expression (i.e. no PZ-hydroxide term) failed to accurately predict the rate behavior of

zine/K_2CO_3. Regardless of the mechanism, values relative to one another, that the CO_2–piperazine re- in water is much faster than the CO_2–MEA reaction. ionally, the piperazine rate is increased over its value er in the presence of aqueous potassium carbonate.

nclusions

erazine is an effective promoter of CO_2 absorption in us potassium carbonate. Rates comparable to those n 7 m MEA are achieved in a 20 wt% K_2CO_3 solution ted with 0.6 m piperazine.

del predictions indicate that capacity is somewhat in- dent of PZ concentration; conversely, an increase in ium carbonate yields a large increase in capacity. A ity comparison with 7 m MEA and 1.2 m PZ/8.5 m A reveals that a 20 wt% K_2CO_3 is not competitive. A % K_2CO_3 solution approaches the capacity of MEA.

alysis of equilibrium data indicates that the heat of tion of CO_2 increases with the addition of PZ to us potassium carbonate. Values for ΔH_{abs} vary from al/mol (Tosh et al., 1959) in 20 wt% K_2CO_3 to cal/mol for a 0.6 m PZ/20 wt% K_2CO_3.

ton NMR suggests that piperazine carbamate is the ant species at high loading. Consequently, it is re- ible for most of the reaction rate. Given that piperazine much faster than the carbamate, it can be concluded ading has a significant effect on absorption rates.

ng regression data from the rate model, the appar- te constant of piperazine in 20 wt% K_2CO_3 is ap- nately five times faster than in water. The apparent onstant for piperazine carbamate is the same as in MDEA. The apparent rate constant for piperazine in 5 M hydroxide/3.6 m K^+ solution is 22 times faster n water, emphasizing the suspected catalytic effects of on CO_2 absorption. For interpretation as an actual rate nt, a rigorous analysis of the absorption is needed to nt for effects of instantaneous flux.

erazine is an effective additive in that it substantially ses the absorption rate of CO_2. Current studies re- hat, coupled with the low heat of absorption associ- vith aqueous K_2CO_3, the PZ/K_2CO_3 system could po- lly reduce energy costs associated with CO_2 removal. panded study of the solvent over a broader range of trially significant conditions is warranted. A rigorous odynamic model will be necessary to encompass the ded solvent concentrations and conditions.

owledgements

is research was supported by the Separations Research am at The University of Texas at Austin and The Texas nced Technology Program.

References

Astarita, G., 1961. Carbon dioxide absorption in aqueous ethanolamine solutions. Chemical Engineering Science 16, 202–207.

Astarita, G., Savage, D.W., Bisio, A., 1983. Gas treating with chemical solvents. Wiley, New York.

Benson, H.E., Field, J.H., Jimeson, R.M., 1954. CO_2 absorption employing hot potassium carbonate solutions. Chemical Engineering Progress 50 (7), 356–364.

Benson, H.E., Field, J.H., Haynes, W.P., 1956. Improved process for CO_2 absorption uses hot carbonate solutions. Chemical Engineering Progress 52 (10), 433–438.

Bishnoi, S., 2000. Carbon dioxide absorption and solution equilibrium in piperazine activated methyldiethanolamine. Ph.D. Thesis, The University of Texas at Austin, Austin, TX.

Bosch, H., Versteeg, G.F., Van Swaaij, W.P.M., 1989a. Gas–liquid mass transfer with parallel reversible reactions–III. Absorption of CO_2 into solutions of blends of amines. Chemical Engineering Science 44 (11), 2745–2750.

Bosch, H., Versteeg, G.F., Van Swaaij, W.P.M., 1989b. Gas–liquid mass transfer with parallel reversible reactions–II. Absorption of CO_2 into amine-promoted carbonate solutions. Chemical Engineering Science 44 (11), 2735–2743.

Caplow, M., 1968. Kinetics of carbamate formation and breakdown. Journal of the American Chemical Society 90 (24), 6795–6803.

Caracotsios, M., 1986. Model parametric sensitivity analysis and nonlinear parameter estimation. Theory and applications. Ph.D. Thesis, The University of Wisconsin, Madison, WI.

Cullinane, J.T., 2002. Carbon dioxide absorption in aqueous mixtures of potassium carbonate and piperazine. M.S. Thesis, The University of Texas at Austin, Austin, TX.

Danckwerts, P.V., 1970. Gas–Liquid Reactions. Carberry, J.J. (Ed.), McGraw-Hill, New York.

Dang, H., 2001. CO_2 absorption rate and solubility in monoethanolamine/piperazine/water. M.S. Thesis, The University of Texas at Austin, Austin, TX.

Edwards, T., Maurer, G., Newman, J., Prausnitz, J., 1978. Vapor–liquid equilibria in multicomponent aqueous solutions of volatile weak electrolytes. A.I.Ch.E. Journal 24 (6), 966–976.

Glasscock, D.A., 1990. Modeling and experimental study of carbon dioxide absorption into aqueous alkanolamines. Ph.D. Thesis, The University of Texas at Austin, Austin, TX.

Laddha, S.S., Danckwerts, P.V., 1982. The absorption of CO_2 by amine-potash solutions. Chemical Engineering Science 37 (5), 665–667.

Pacheco, M.A., 1998. Mass transfer, kinetics and rate-based modeling of reactive absorption. Ph.D. Thesis, The University of Texas at Austin, Austin, TX.

Pagano, J.M., Goldberg, D.E., Fernelius, W.C., 1961. A thermodynamic study of homopiperazine, piperazine, and n-(2-aminoethyl)-piperazine and their complexes with copper(II) ion. Journal of Physical Chemistry 65, 1062.

Pohorecki, R., Xoan, D.T., Moniuk, W., 1988. Study of carbon dioxide absorption in aqueous solution of potassium carbonate containing ethylaminoethanol. II. Kinetic relations for 2-(ethylamino)ethanol. Inzynieria Chemieczna Procesowa 9 (4), 667–680.

Posey, M.L., 1996. Thermodynamics model for acid gas loaded aqueous alkanolamine solutions. Ph.D. Thesis, The University of Texas at Austin, Austin, TX.

Sartori, G., Savage, D.W., 1983. Sterically hindered amines for CO_2 removal from gases. Industrial and Engineering Chemistry Fundamentals 22, 239–249.

Savage, D.W., Sartori, G., 1984. Amines as rate promoters for carbon dioxide hydrolysis. Faraday Discussions of the Chemical Society 77, 17–31.

I.S., Field, J.H., Benson, H.E., Haynes, W.P., 1959. Equilibrium y of the system potassium carbonate, potassium bicarbonate, carbon ide, and water. United States Bureau of Mines, 5484.

P.C., Ho, W.S., Savage, D.W., 1988. Carbon dioxide absorption promoted carbonate solutions. A.I.Ch.E. Journal 34 (6), –931.

Versteeg, G.F., van Swaaij, W.P.M., 1988. Solubility and Diffusivity of Acid Gases (CO_2, N_2O) in Aqueous Alkanolamine Solutions. Journal of Chemical Engineering Data 33 (1), 29–34.

Available online at www.sciencedirect.com
SCIENCE DIRECT®
Chemical Engineering and Processing 43 (2004) 857–865
Chemical Engineering and Processing
www.elsevier.com/locate/cep

Enhanced carbon dioxide removal by promoted hot potassium carbonate in a split-flow absorber

M.R. Rahimpour*, A.Z. Kashkooli

Department of Chemical Engineering, Shiraz University, Shiraz, P.O. Box 71345, Shiraz, Iran

Received 4 February 2003; received in revised form 9 May 2003; accepted 30 May 2003

ct

is work, a comprehensive model has been developed for the absorption of carbon dioxide into promoted hot potassium carbonate n. The model, which is based on penetration theory, incorporates an extensive set of important reactions and takes into account the ıg between mass transfer and chemical kinetics. The penetration theory provides an appropriate absorption rate and enhancement factor chemical absorption. Operating data for carbon dioxide absorption into DEA–hot potassium carbonate solution has been compared odel predictions. The impact of parameters such inlet temperature of lean solution, promoter concentration, liquid split fraction, hot cation and type of promoter on the performance of a split-flow absorber have been examined. The use of other promoters is an efficient enhance the carbon dioxide absorption, which has been discussed in this paper.

ds: Hot potassium carbonate; Split-flow absorber; Carbon dioxide absorption; Promoters; Enhanced absorption

roduction

separation of carbon dioxide from mixtures with other is a process of substantial industrial importance. In the acture of ammonia from hydrocarbons or coal feeds, moval of carbon dioxide from the synthesis gas is a process step. Large volumes of natural gas are also l for carbon dioxide removal. Several processes are in r CO_2 removal but process selection must be based nomic and clean-up ability. Among the processes, the promoted hot carbonate process provides an economic ficient way for removing large quantities of CO_2 from sis gases. In this process, the amine generally provide bsorption rate, while the carbonate–bicarbonate buffer advantages of large capacity for CO_2 and ease of eration.

hot carbonated process was originally developed by n et al. [1], and has since undergone several improve- [2–4]. The most important improvement is the dis- that small amount of certain organic or inorganic ad- s (promoters) can enhance the absorption rate largely [5]. The concept of the addition of amine to carbonate system to enhance CO_2 absorption has been known for a long time [6,7].

In the mechanism, which is called homogeneous catalysis, the promoter first forms an intermediate with CO_2 and the intermediate is then hydrolyzed to produce the final product, bicarbonate [5]. In another mechanism, which is called shuttle, the promoter acts as a carrier to provide an additional pathway for the transport of CO_2 from the gas–liquid interface to the bulk liquid [7]. Astarita et al. [8] concluded that the two mechanisms are different only quantitatively, not qualitatively. Savage and Astarita [9] indicated that the rate promotion effect of amine in carbonate solutions could be described very well from the viewpoint of homogeneous catalysis at higher temperatures in the range of industrial operating conditions. In a recent study [10], the joint action of two promoters on the absorption of CO_2 in alkaline buffer solution measured experimentally.

A number of authors already investigated the modeling and simulation of hot potassium carbonate process [11,12], but the published information is very little detailed. The recent model proposed by Sanyal et al. [11] for an industrial hot potassium carbonate process, simplified the calculations and gave reasonable predictions but it did not consider the effect of chemical reactions on CO_2 absorption and neglected

rresponding author. Tel.: +98-711-2303-071;
8-711-6287-294.
ail address: rahimpor@shirazu.ac.ir (M.R. Rahimpour).

1016/S0255-2701(03)00106-5

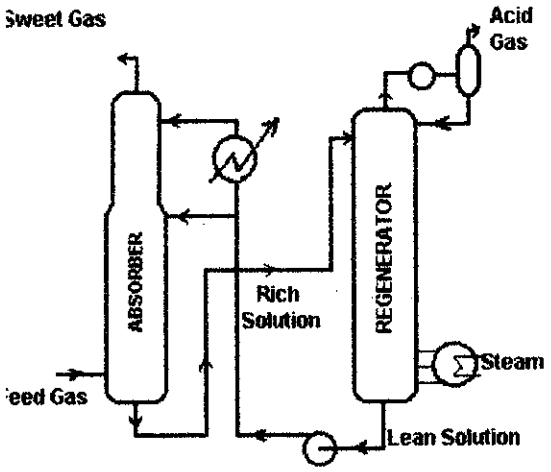

. Schematic diagram of a conventional split-flow absorber-stripper ement.

ffect of amine concentration on the absorption perfor- :e. However, no previous work has examined the be- ɔr and types of promoters in the split-flow absorber and fications of split-stream or attempted to exploit this be- ɔr to develop better process. Therefore, we decided to ' more thoroughly the effect of these parameters on the ɔn dioxide absorption with potassium carbonate.

this work a general model for the mass transfer/reaction :sses in carbon dioxide absorber using promoted hot ısium carbonate has been developed. The combined ef- ɔf mass transfer and chemical reaction was treated by ce-renewal penetration theory. The effect of different neters on the performance of a split-flow absorber has investigated and the design consequences of different ɪns have been discussed.

rocess description

g. 1 shows a schematic diagram of a conventional flow absorber-stripper [13]. The process scheme is simple, the feed gas is contacted counter-currently the hot potassium carbonate in the absorber, and es- ally all of the carbon dioxide is removed. The effluent n which contains only a very small amount of carbon ide can be used in ammonia synthesis. The rich solution ɔd with carbon dioxide passes to the regenerator where stripped by counter-current contacting with a stream of ping steam. A portion of lean solution from the regen- r is cooled and fed into the top of the absorber while najor portion is added at a point some distance below op without any changing in temperature. This simple ification, which is called split-flow process, improves ɪurity of the product gas by decreasing the equilibrium r pressure of the CO_2 over the portion of solution last ıcted by the gas. Tables 1 and 2 show the characteristics ro absorption columns.

Table 1
Characteristics of the absorption tower, packing and system for CO_2 absorption for the first column [13]

Parameters	Top section	Bottom section	Units
Height of packing	19.84	21	m
Diameter of packed bed	3.4	4.5	m
Packing size (d_p)	51	47	mm
Packing shape	Metal mini rings	Metal mini rings	–
Specific surface of packing (a)	123	144	m^{-1}
Packing void fraction	0.975	0.878	–

3. Chemical reactions

The basic reaction chemistry for aqueous hot potassium carbonate solution and CO_2 is represented by the following reversible reaction [8]:

$$CO_2 + K_2CO_3 + H_2O \leftrightarrow 2KHCO_3 \quad (1)$$

Since potassium carbonate and bicarbonate are both strong electrolytes, it may be assumed that the metal is present only in the form of K^+ ions, so reaction (1) may be more realistically represented in the ionic terms as:

$$CO_2 + CO_3^{2-} + H_2O \leftrightarrow 2HCO_3^- \quad (2)$$

The above reaction is evidently made up of a sequence of elementary steps. The carbonate ion first reacts with water to generate hydroxyl ions, which then react with CO_2 as follows [8]:

$$CO_3^{2-} + H_2O \leftrightarrow HCO_3^- + OH^- \quad (3)$$

$$CO_2 + OH^- \leftrightarrow HCO_3^- \quad (4)$$

Since reaction (3) is instantaneous reaction, reaction (4) is the rate-controlling step, so that the rate equation for reaction of carbon dioxide with un-promoted hot potassium carbonate leads to [8,14]:

$$r_{OH} = k_{OH}[OH^-][CO_2] - k_{-OH}[HCO_3^-] \quad (5)$$

where k_{OH} and k_{-OH} are forward and backward rate constants of reaction (4).At equilibrium condition Eq. (5) gives:

$$k_{-OH}[HCO_3^-] = k_{OH}[OH^-][CO_2]_e \quad (6)$$

Table 2
Characteristics of the absorption tower, packing and system for CO_2 absorption for the second column [11]

Parameters	Column specifications	Units
Height of packing	17.2	m
Diameter of packed bed	1.4	m
Packing size (d_p)	37	mm
Packing shape	Intalox saddles (ceramic)	–
Specific surface of packing (a)	144	m^{-1}
Packing void fraction	0.80	–

$CO_2]_e$ is the equilibrium concentration of CO_2. The ion for reverse reaction (4) in Eq. (6) has been eval- ›y considering conditions at equilibrium, but it is ly true, even when the system is not at equilibrium].Substituting Eq. (6) into Eq. (5) gives [14]:

$$(k_{OH}[OH^-])([CO_2] - [CO_2]_e) \quad (7)$$

ate–bicarbonate system is a buffer solution, so the tration of OH^- ion in the solution near the surface of s not significantly depleted by the absorbed CO_2. In e, the carbon dioxide undergoes a pseudo-first order ı and Eq. (7) may be rewritten as [8,14,15]:

$$k_1([CO_2] - [CO_2]_e) \quad (8)$$

k_1 denotes apparent first-order rate constant.

n a small amount of amine is added into the solution, orption rate of carbon dioxide is enhanced greatly ng to the following reactions [8]:

$$\underset{\text{(Amine)}}{RR'NH} \leftrightarrow \underset{\text{(Carbamate)}}{RR'NCOOH} \quad (9)$$

$$\underset{\text{nate)}}{OOH} + OH^- \leftrightarrow HCO_3^- + \underset{\text{(Amine)}}{RR'NH} \quad (10)$$

gher temperatures in the range of industrial operating ons, the rate of reaction (10) increases significantly, is better represented by the homogeneous catalychanism [15,8], and reaction (9) is rate-controlling sing the same approach for deriving Eq. (8), gives owing pseudo-first order rate equation for r_{Am} [14]:

$$(k_{Am}[Am])([CO_2] - [CO_2]_e)$$
$$k_2([CO_2] - [CO_2]_e) \quad (11)$$

k_2 is apparent first-order rate constant.

ing Eqs. (7) and (11) leads to the overall pseudo-first ate equation of carbon dioxide with promoted hot um carbonate in liquid phase:

$$_{OH}[OH^-] + k_{Am}[Am])([CO_2] - [CO_2]_e)$$
$$CO_2] - [CO_2]_e) \quad (12)$$

k is the overall apparent first-order rate constant and ıed as:

$$_{OH}[OH^-] + k_{Am}[Am]) \quad (13)$$

del development

ing material and energy balance around a differential of column shown in Fig. 2, gives the mathematical of a packed absorber [17]. Envelope III is an ele- volume in the differential packed height (ΔZ) of the er, consisting of the gas and liquid phase denoted by ›es I and II, respectively. The major assumptions are ıdy-state conditions prevail, (2) pressure drop across ›ked bed is negligible, and (3) CO_2 and H_2O are the ›mponents transported across the interface.

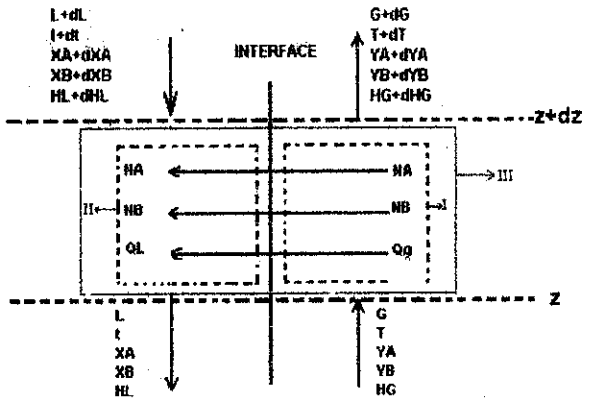

Fig. 2. Differential section of packed absorber.

4.1. Mole balance

4.1.1. Gas phase

A differential mole balance in the gas phase around Δz gives a differential equation for gas flow along the bed:

$$\frac{dG}{dz} = -(N_{CO_2} + N_{H_2O})a \quad (14)$$

where G is superficial molar velocity of gas; N_{CO_2} and N_{H_2O} are mass transfer fluxes of CO_2 and water, and a is the specific surface area of packing.

A differential mole balance in gas phase for CO_2 and water gives the following differential equations for mole fraction of carbon dioxide and water in the gas phase:

$$\frac{dy_{CO_2}}{dz} = \frac{[(N_{H_2O}y_{CO_2} - N_{CO_2}(1 - y_{CO_2}))]a}{G} \quad (15)$$

$$\frac{dy_{H_2O}}{dz} = \frac{[(N_{CO_2}y_{H_2O} - N_{H_2O}(1 - y_{H_2O})]a}{G} \quad (16)$$

4.1.2. Liquid phase

Here it has been assumed that for the amine-promoted carbonate solution the reaction is fast and hence the reaction takes place at the same rate at which the carbon dioxide is reached to reactants in each element of liquid [12,14]. Therefore, we can develop the differential equation for molar flow rate and compositions of liquid phase when the rate of absorption and stoichiometry of reaction (1) are taken into account.

A differential mole balance in liquid phase gives an equation for liquid flow rate as follows:

$$\frac{dL}{dz} = -N_{H_2O}a \quad (17)$$

where L is the superficial molar velocity of liquid.

In the liquid phase, K_2CO_3 consumed by chemical reaction as the solution moves down the packing bed. Hence, when the reaction stoichiometry is taken into account, differential moles balance for K_2CO_3 gives:

$$\frac{d(Lx_{K_2CO_3})}{dz} = N_{CO_2}a \quad (18)$$

ıcing dL by Eq. (17) gives rise to the following differ- equation for mole fraction of K_2CO_3:

$$\frac{CO_3}{} = \frac{[N_{H_2O}x_{K_2CO_3} + N_{CO_2}]a}{L} \quad (19)$$

ıce $KHCO_3$ is the reaction product in the liquid phase, ın develop the differential equation for mole fraction HCO_3, when the reaction stoichiometry is taken into ınt:

$$\frac{CO_3}{z} = \frac{[N_{H_2O}x_{KHCO_3} - 2N_{CO_2}]a}{L} \quad (20)$$

balance for H_2O also yields the following equation in quid phase:

$$\frac{O}{} = \frac{[N_{CO_2} - N_{H_2O}(1 - x_{H_2O})]a}{L} \quad (21)$$

Energy balance

differential energy balance for the gas phase around ifferential height of packed bed (dz), gives rise to the wing differential equation for temperature of gas phase:

$$= \frac{(N_{CO_2} + N_{H_2O})a}{G} T - \frac{(N_{CO_2}C_{P_{CO_2}} + N_{H_2O}C_{P_{H_2O}})a}{GC_{P_G}} T - \frac{h_g a(T - t)}{GC_{P_G}} \quad (22)$$

e the heat effects due to bulk motion, mass transfer and ection between phases are taken into account [11]. milarly, an energy balance in the liquid phase gives o the following differential equation for temperature of l phase:

$$= \frac{N_{H_2O}a}{L} t - \frac{(N_{CO_2}C_{P_{CO_2}} + N_{H_2O}C_{P_{H_2O}})a}{LC_{P_L}} T - \frac{h_g a(T - t)}{LC_{P_L}} - \frac{(N_{CO_2}\Delta H_{CO_2} + N_{H_2O}\Delta H_{H_2O})a}{LC_{P_L}} \quad (23)$$

e ΔH_{CO_2} is heat of absorption and reaction of CO_2, ΔH_{H_2O} is heat of vaporization of water [11].

Mass transfer

ıe combined effect of chemical reaction presented by 12) and mass transfer are conveniently and adequately ed by the framework of penetration-surface renewal the- leveloped by Danckwerts [14]. The absorption rate of on dioxide in the liquid phase according to this theory homogeneous catalysis mechanism can be expressed as ws [14–16]:

$$_2 = Ek_L(C_{CO_{2_i}} - C_{CO_{2_e}}) \quad (24)$$

re $C_{CO_{2_i}}$ is the concentration of carbon dioxide at the face and $C_{CO_{2_e}}$ is the equilibrium concentration of unreacted carbon dioxide in the bulk of liquid when the reverse reaction of carbon dioxide is appreciable. k_L is liquid phase mass transfer coefficient and E is the enhancement factor and describes the mass transfer coupled by chemical reactions as follows [14]:

$$E = \sqrt{1 + \frac{D_{CO_2}k}{k_L^2}} \quad (25)$$

where k is defined by Eq. (13).The rate of absorption, which is defined by Eq. (24), can be rewritten in terms of physical solubility of carbon dioxide in solution, H, in the reactive K_2CO_3 solution as:

$$N_{CO_2} = k_L HE(P_{CO_{2_i}} - P_{CO_{2_e}}) \quad (26)$$

The rate of mass transfer of carbon dioxide in the gas phase is also as follows:

$$N_{CO_2} = k_{g_{CO_2}}(P_{CO_2} - P_{CO_{2_i}}) \quad (27)$$

where $k_{g_{CO_2}}$ is gas phase mass transfer coefficient of carbon dioxide.

Combining Eqs. (26) and (27) and eliminating the interface partial pressure of carbon dioxide, $P_{CO_{2_i}}$, gives rise to the following equation for the absorption rate:

$$N_{CO_2} = \left(\frac{k_{g_{CO_2}}k_L EH}{k_{g_{CO_2}} + k_L EH}\right)(P_{CO_2} - P_{CO_{2_e}}) = K_{g_{CO_2}}(P_{CO_2} - P_{CO_{2_e}}) \quad (28)$$

where $K_{g_{CO_2}}$ is overall gas phase mass transfer coefficient of carbon dioxide.

Water is another component, which substantially transported in gas phase across the interface. It may be assumed that there is no liquid-side resistance for the mass transfer of the solvent water vapor. Therefore, the overall mass transfer coefficient for the water vapor is the same as the mass transfer coefficient in gas phase, and then the mass transfer rate of water per unit interfacial area is:

$$N_{H_2O} = K_{g_{H_2O}}(P_{H_2O} - P_{H_2O_e}) \quad (29)$$

where $K_{g_{H_2O}}$ is overall gas phase mass transfer coefficient of water.

4.4. Equilibrium, kinetic and transport parameters

The kinetic parameters of different amines are provided in Table 3 and the equilibrium and transport parameters are tabulated in Table 4.

5. Numerical solution

The proposed nine differential Eqs. (14)–(17) and Eqs. (19)–(23), need to be solved to simulate a column of

stants of reaction between amines and CO_2 where t is liquid ıre (K) [16]

	k_{Am} (m^3 $kmol^{-1}$ h^{-1})
	$6.4 \times 10^8 \exp\left[14.97\left(1-\frac{353}{t}\right)\right]$
	$3.4 \times 10^8 \exp\left[13.54\left(1-\frac{353}{t}\right)\right]$
	$12 \times 10^8 \exp\left[13.40\left(1-\frac{353}{t}\right)\right]$

height by taking into account the boundary condi- he flow rate, composition and temperature of the gas ıntering the column at its bottom and the flow rate, ıration and temperature of the liquid phase entering ımn at its top are known in simulation problem. To ɜ integration procedure, the flow rate, concentration nperature of the liquid phase at the bottom of the need to be estimated. With the help of the estimated

um, kinetics and transport parameters

r Expression	Source
$\alpha = \frac{[K^+]-2[CO_3^{2-}]}{[K^+]} = \frac{[HCO_3^-]}{[K^-]}$	[15]
$P_{CO_{2e}} = 2\frac{K_2[K^+]}{K_1H}\frac{\alpha^2}{1-\alpha}$	[15]
$\log(K_1) = -(3404.7/t)+14.843-0.03279t$	[15]
$\log(K_2) = -(2902.4/t)+6.498-0.0238t$	[15]
$\log(H/H_W) = -K_SI$; $K_S = 0.06$, $I = 6.2$	[15]
$\log H_W = (1140/t)-5.30$	[15]
$\log P_{H_2O_e} = -(L'/2.303R)((1/t)-2.45\times10^{-3})$ $-1.1672+C$; $L' = 40\,983.6$	[18]
$C = 1.2014+(0.2857/x_c)-(0.0537/x_c^2)$	[18]
$x_C = \frac{0.691(\%KHCO_3)}{\%K_2CO_3+0.691(\%KHCO_3)}$	[18]
$\log(k_{OH}) = 13.635-(2895/t)+0.08I$	[19]
$\frac{k_{g_k}RT}{aD_{g_k}} = 5.32\left(\frac{\hat{G}}{a\mu_g}\right)^{0.7}\left(\frac{\mu_g}{\rho_gD_{g_k}}\right)^{1/3}(ad_p)^{-2.0}$	[14]
$k_L\left(\frac{\mu_l^2}{\rho_l^2g}\right)^{1/3}/D_{CO_2} = 0.015\left(\frac{\hat{L}}{a\mu_l}\right)\left(\frac{\mu_l}{\rho_lD_{CO_2}}\right)^{1/3}$	[20]
$\log D_{CO_2} = -3.0188-\frac{586.9729}{t}-0.4437$	[21]
$h_g = \sum_k y_kh_{g_k}$	[22]
$h_{g_k} = k_{y_k}C_{p_k}(Le)^{2/3}$	[22]
$C'_{P_L} = 4.1774-0.0382\omega-0.4445\times10^{-3}\omega^2$ $+1.2798\times10^{-5}\omega^3$	[24]
$\Delta H_{CO_2} = 27\,228.2+81.37\omega+5.32\omega^2-0.1313\omega^3$ $+1.654\times10^{-3}\omega^4$	[23]
$\omega = \frac{\%K_2CO_3+0.691(\%KHCO_3)}{\%K_2CO_3+0.781(\%KHCO_3)+\%H_2O}$	[11]

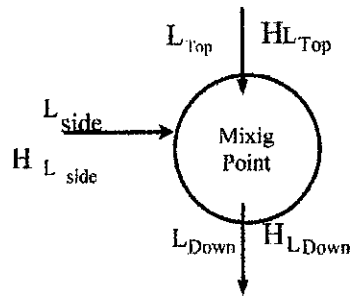

Fig. 3. Schematic diagram of mixing point between split-flow and downward liquid stream.

values, the column equations can be integrated by using the Euler method up to the top point where the split hot lean solution is added to the column. At this point the following equations, which are the results of mass and energy balance at the mixing point, are used to calculate molar flow rate, composition and temperature of the liquid stream in the next upper increment as follows:

$$L_{Top} = L_{Down} - L_{Side} \tag{30}$$

$$x_{Top} = \frac{L_{Down}x_{Down} - L_{Side}x_{Side}}{L_{Top}} \tag{31}$$

$$T_{L_{Top}} = \frac{L_{Down}C_{PL_{Down}}T_{L_{Down}} - L_{Side}C_{PL_{Side}}T_{L_{Side}}}{L_{Top}C_{PL_{Top}}} \tag{32}$$

in which *Down* denotes the stream below mixing point, *Top* denotes the stream above mixing point and subscript *Side* represents the side feed stream as shown in Fig. 3.

The numerical procedure is continued from mixing point up to the top of the column to obtain actual values of liquid entering, with the help of which further iteration can be made using shooting method until satisfactory convergence is obtained [25–27]. In this method two values for the liquid flow rate at the bottom, $L_b^{(1)}$ and $L_b^{(2)}$, are assumed and the corresponding values for the liquid flow rates at the top, $L_t^{(1)}$ and $L_t^{(2)}$, are calculated by the model. The points A and B are plotted at $(L_b^{(1)}, L_t - L_t^{(1)})$ and $(L_b^{(2)}, L_t - L_t^{(2)})$ in a xy plane, where L_t is the observed liquid flow rate at the top. Line AB is extended to intersect the x axis at C, which provides the next guess for L_b say $L_b^{(3)}$ [27].

The remaining six variables, liquid temperature, t, and liquid mole fractions, $x_{K_2CO_3}$, x_{KHCO_3}, x_{H_2O}, x_{DEA} and x_{KVO_3} are treated in the same manner. A computer program to solve the model equations was written in FORTRAN language.

6. Model validation

A verification of the model was carried out by comparison with the operating data of hot carbonate process, under the design specification for two different columns summarized in Table 1 from Shiraz Petrochemical Complex [13] and Table 2 from data reported by Sanyal et al. [11]. The

5
ırison of calculated results with the observed plant data [13] with :ation indicated in Table 1 for the first column

:ters	Inlet	Outlet		Error (%)
		Observed	Calculated	
ıemperature (K)				
	343.2	388.2	394.6	−1.69
	401.0			
flow rate (kmol h^{-1})				
	15 418.7	63 660.2	62 117.1	2.42
	46 259.6			
composition (mole fraction)				
;	0.03663	0.01260	0.01331	−5.63
';3	0.02527	0.07110	0.07121	−0.15
	0.92943	0.90766	0.90689	0.08
	0.00722	0.00720	0.00715	0.69
(anti-corrosion)	0.00145	0.00144	0.00144	0.00
mperature (K)	388.2	343.2	357.2	−4.09
ow rate (kmol h^{-1})	8459.0	6660.0	6576.6	1.25
omposition (mole fraction)				
	0.17150	0.00197	0.00199	−1.03
	0.00187	0.00241	0.00241	−0.19
	0.00376	0.00483	0.00484	−0.18
	0.57510	0.73910	0.73964	−0.09
	0.18590	0.23850	0.23910	−0.25
	0.00224	0.00285	0.00288	−0.88
	0.05970	0.01081	0.01002	7.41

cted results and actual data are presented in Tables 5 ;. Overall, for all the cases the obtained agreement is 'actory.

7. Results and discussion

The performance of the carbon dioxide absorption was investigated by conducting absorption simulations over some runs under the design and operating conditions summarized in Tables 1 and 5 for the first column. The simulation results were plotted as profiles of the dependent parameters versus independent variables, along with plant data. In addition, the effects of different parameters on the absorption performance were investigated.

7.1. Effect of promoter concentration

According to Fig. 4, an increase in the amine concentration first induces a higher CO_2 removal while raising the amine content beyond a specific amount has no effect on the exit CO_2 concentration. The possible explanation for this behavior is that increasing the amine concentration reflects the higher enhancement factor in the liquid phase, which is directly proportional to the overall K_g in the case of liquid-phase controlled mass transfer. With more increasing the amine concentration, the gas phase mass transfer is considered the major factor controlling the absorption process so the CO_2 removal is unaffected by increasing the promoter concentration.

7.2. Effect of promoter type

The role of amine type in carbon dioxide removal is shown in Fig. 5. Three types of promoter were compared

6
ırison of calculated results with the observed plant data [11] with specification indicated in Table 2 for the second column

eters	Inlet	Outlet		Error (%)
		Observed	Calculated	
' *temperature (K)*				
	343.0	392.0	379.0	3.32
	371.0			
' *flow rate (kmol h^{-1})*				
	2630.0	5308.0	5350.5	−0.80
	2630.0			
' *composition (mole fraction)*				
3	0.04013	0.015800	0.01579	0.08
';3	0.02015	0.066300	0.06711	−1.22
	0.93200	0.919800	0.90949	1.12
	0.00719	0.007005	0.00712	−1.62
(anti-corrosion)	0.00055	0.000540	0.00055	−1.80
ow rate (kmol h^{-1}) with inlet temperature 408 K	762.9	547.1	545.1	0.36
omposition (mole fraction)				
	0.16590	0.00100	0.00091	8.73
	0.00184	0.00257	0.00258	−0.20
	0.00263	0.00366	0.00368	−0.57
	0.53060	0.73880	0.74260	−0.51
	0.17330	0.24130	0.24254	−0.51
	0.00210	0.00290	0.00294	−1.35
	0.12370	0.00990	0.00879	11.22

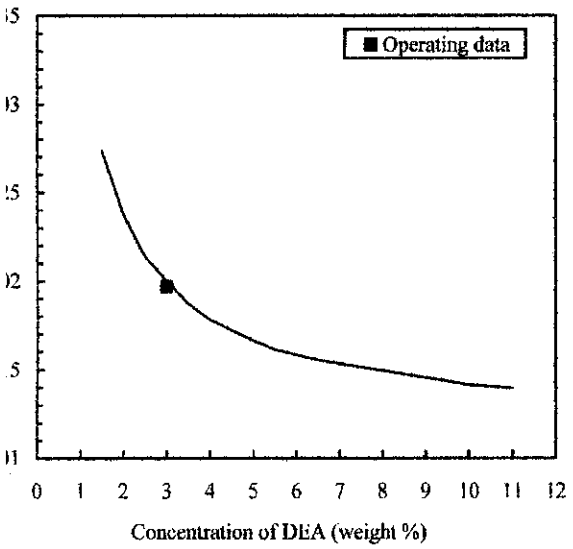

:xit CO_2 concentration versus the weight percent of amine in tion.

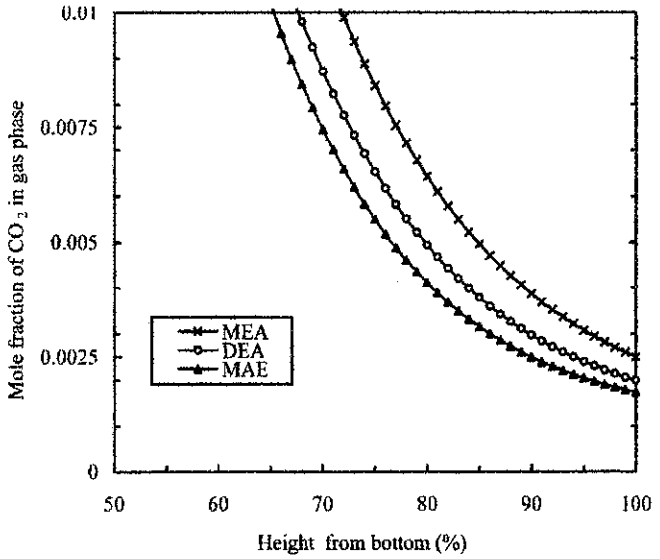

Fig. 5. Exit CO_2 concentration profiles along the packed bed height for various promoters.

r effectiveness in carbon dioxide removal at identical ıg conditions; DEA, MEA and methyl amino ethanol . From this figure, MAE provides more absorption EA and MEA. The difference between the CO_2 re- ıfficiency by the three types of amines is preliminary :ed by second-order rate constant, k_{Am} as provided : 3.

'ect of liquid split fraction

ılit-stream absorption systems, the carbon dioxide l behavior is further complicated by the presence liquid side feed. In this system a fraction of the ılution from regenerator is cooled and fed at the tion of absorber. As it is clearly demonstrated in an increase in this stream would result in a higher ıf synthesis gas, due to the lowering vapor pressure at lower temperature. As this fraction increases, :tion of hot lean solution fed at middle of column es which would results lower temperature at the section of column. However, in this case, the influ- overall mass transfer coefficient seems to dominate e driving force, thus results to less sensitivity of dioxide removal to the increase in cold liquid split ı.

'ect of liquid temperature

temperature of lean solution also has an influence absorption performance as demonstrated in Fig. 7. ;ure indicates the higher mass-transfer performance r temperature, which can be presented by decreasing ilibrium vapor pressure of CO_2 over the portion of ı last contacted by the gas. It is clear that as we attain :oncentrations, the absorber curves A and B have a horizontal asymptote, so a large decrease in the inlet liquid temperature is required to obtain a small reduction in outlet carbon dioxide concentration. Hence, beside the influence of the equilibrium vapor pressure of CO_2, the overall mass transfer coefficient, which depends on temperature directly, plays an important role on the absorption performance.

7.5. Effect of hot split-stream

A change in the location of the entering hot stream has an effect on the concentration of CO_2 in exit gas stream as shown in Fig. 8. The change of hot split-stream location primary affects liquid flow rate profile, which would result

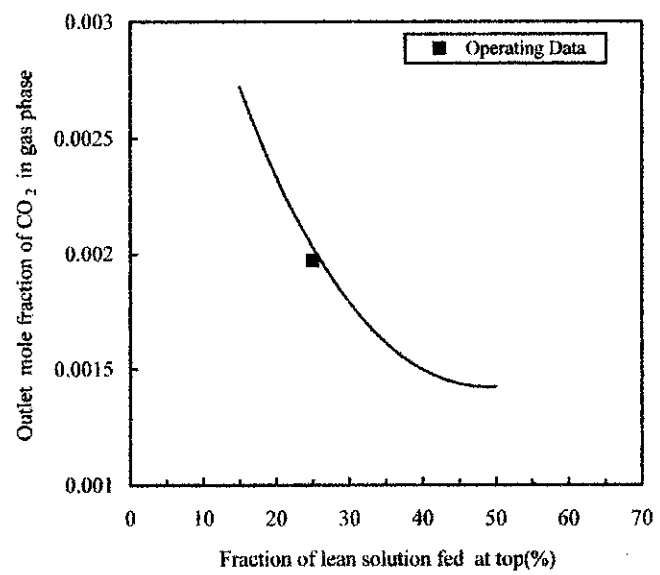

Fig. 6. Exit CO_2 concentration vs. fraction of lean solution fed at the top of column.

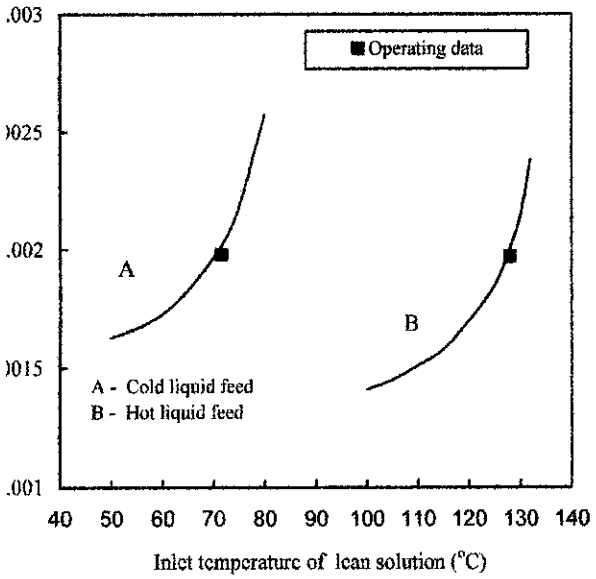

7. Exit CO_2 concentration vs. inlet temperature of lean solution.

ges in liquid temperature and mass transfers coefficient es. An interesting feature of this figure is that we usu- observe a point of minimum carbon dioxide removal. arises at the transition between two region of column tion, i.e. that in as location of hot side feed moves the column allows lower liquid temperature at top n which would result in higher mass transfer perfor- e by decreasing the vapor pressure of carbon dioxide, hat in which as the location of hot side feed moves lows higher liquid temperature and flow rate at bottom n would result in higher mass transfer performance creasing overall mass transfer coefficient. Therefore, ot feed location from bottom must be chosen in order lize this compromise.

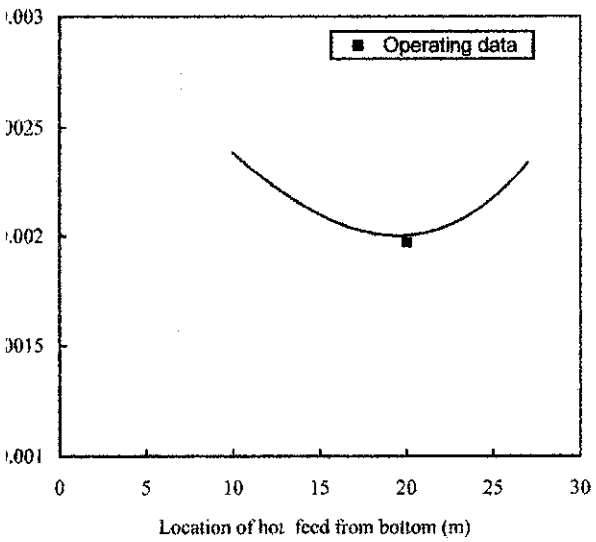

. Exit CO_2 concentration vs. location of hot split-stream location.

8. Conclusion

The model presented in this work, accurately predicted absorber performance when the results were compared with operating data. The results indicate the performance of hot potassium carbonate process can be improved by finding better process systems. Judicious selection of the inlet split-streams temperature, hot split-stream location, and ratio of the cold feed rate to the hot feed rate can, therefore, lead to design that achieve high carbon dioxide removal. Promoter type is considered as another essential factor affecting the efficiency of CO_2 absorption process. The use of other amines is an efficient way to enhance the separation, which has been addressed in this paper. The model provides a procedure to investigate the effect of new promoters on the CO_2 absorption.

Acknowledgements

The authors gratefully acknowledge the financial support of Shiraz Petrochemical Complex.

Appendix A. Nomenclature

a	specific surface area ($m^2\ m^{-3}$)
C_k	concentration of kth component (kmol m^{-3})
C_{ke}	equilibrium concentration of kth component in the bulk of liquid (kmol m^{-3})
C_{ki}	concentration of kth component at interface (kmol m^{-3})
C_{PG}	molar specific heat of gas (kJ $kmol^{-1}\ K^{-1}$)
C_{PK}	specific heat of kth component (kJ $kmol^{-1}\ K^{-1}$)
C_{pL}	molar specific heat of liquid (kJ $kmol^{-1}\ K^{-1}$)
C'_{pL}	specific heat of liquid (kJ $kg^{-1}\ K^{-1}$)
D_{CO_2}	diffusivity of CO_2 in K_2CO_3 solution ($m^2\ h^{-1}$)
D_{gCO_2}	diffusivity of CO_2 in gas ($m^2\ h^{-1}$)
d_p	packing nominal size (m)
E	enhancement factor
G	molar velocity of gas (kmol $m^{-2}\ h^{-1}$)
$\hat{G}$	mass velocity of inert gas (kg $m^{-2}\ h^{-1}$)
H	solubility of carbon dioxide in solution (kmol $atm^{-1}\ m^{-3}$)
h	heat transfer coefficient in gas phase (kJ $m^{-2}\ h^{-1}\ K^{-1}$)
ΔH_{CO_2}	heat of reaction and absorption of CO_2 (kJ $kmol^{-1}$)
ΔH_{H_2O}	heat of vaporization of water (kJ $kmol^{-1}$)
I	ionic strength of solution (kg ion m^{-3})
k	pseudo first order rate constant (h^{-1})
k_{Am}	second order rate constant of amine ($m^3\ kmol^{-1}\ h^{-1}$)
k_{OH}	forward rate constant of reaction (4) ($m^3\ kmol^{-1}\ s^{-1}$)

ackward rate constant of reaction (4) (s^{-1})
as side mass transfer coefficient
(mol h^{-1} m^{-2} atm^{-1})
verall mass transfer coefficient
(mol h^{-1} m^{-2} atm^{-1})
as side mass transfer coefficient (kmol h^{-1} m^{-2})
quid side mass transfer coefficient (m h^{-1})
rst ionization constant for carbonic acid
(mol m^{-3})
econd ionization constant for carbonic acid
(mol m^{-3})
olar velocity of liquid (kmol m^{-2} h^{-1})
quid mass flow rate (kg h^{-1})
eat of vaporization of water (kJ $kmol^{-1}$)
ewis number
ass transfer flux of kth component (kmol m^{-2} h^{-1})
artial pressure of kth component in gas phase (atm)
quilibrium vapor pressure of kth component
gas phase (atm)
artial pressure of kth component in the
quid–gas interface (atm)
niversal gas constant (m^3 atm $kmol^{-1}$ K^{-1})
ross sectional area of column (m^2)
as temperature (K)
quid temperature (K)
ole fraction of kth component in the liquid phase
ole fraction of kth component in the gas phase
patial variable along the height of the column (m)

ymbols
arbonation ratio
as phase viscosity (kg m^{-1} h^{-1})
quid phase viscosity (kg m^{-1} h^{-1})
as phase density (kg m^{-3})
quid phase density (kg m^{-3})
tal equivalent weight percent of K_2CO_3

ces

Benson, J.H. Field, R.M. Jimson, CO_2 absorption employing hot ssium carbonate solution, Chem. Eng. Prog. 50 (1954) 356–364.
Benson, J.H. Field, W.P. Haynes, Improved process for CO_2 rption using hot carbonate solution, Chem. Eng. Prog. 52 (1956) -438.
[3] H.E. Benson, J.H. Field, New data for hot carbonate process, Petrol. Refinery 39 (1960) 127–132.
[4] H.E. Benson, R.W. Parish, Improved benfield process, Hydrol. Process. 53 (4) (1974) 81–88.
[5] F.C. Riesenfield, J.F. Mullowney, Giammarco–Vetrocoke processes, Petrol. Refinery 38 (5) (1959) 161–167.
[6] D.H. Killeffer, Promotion of mass transfer in carbonate solution, Ind. Eng. Chem. 29 (1937) 1293–1298.
[7] A.L. Shrier, P.V. Danckwerts, Promotion effect of amines in carbonate solutions at room temperature, Ind. Eng. Chem. 8 (1969) 581–590.
[8] G. Astarita, D.W. Savage, Promotion of CO_2 mass transfer in carbonate solutions, Chem. Eng. Sci. 36 (1981) 581–588.
[9] D.W. Savage, G. Astarita, Amines as rate promoters for carbon dioxide hydrolysis, Faraday Discuss. Chem. Soc. 77 (1984) 17–31.
[10] G. Vazquez, F. Chenlo, G. Periera, Enhancement of the absorption of CO_2 in alkaline buffer solutions: joint action of two enhancer, Ind. Eng. Chem. Res. 38 (1999) 2160–2162.
[11] D. Sanyal, N. Vasishtha, D.N. Saraf, Modeling of carbon dioxide absorber using hot carbonate process, Ind. Eng. Chem. Res. 27 (1988) 2149–2156.
[12] M.M. Suenson, C. Georgakis, L.B. Evans, Steady-state and dynamic modeling of a gas absorber-stripper system, Ind. Eng. Chem. Fundam. 24 (1985) 288–295.
[13] Shiraz Petrochemical Complex, Ammonia Plant, Operating Data of Benfield Process, 2002.
[14] P.V. Danckwerts, Gas–Liquid Reactions, McGraw-Hill, 1970.
[15] P.V. Danckwerts, M.M. Sharma, The absorption of carbon dioxide into solutions of alkalis and amines, Chem. Eng. 44 (1966) 244–280.
[16] E. Leder, The absorption of CO_2 into chemically reactive solutions at high temperature, Chem. Eng. Sci. 26 (1971) 1381–1390.
[17] A.Z. Kashkooli, M.Sc. Thesis, Shiraz University, Shiraz, Iran 2002.
[18] J.S. Tosh, H.E. Benson, J.H. Field, Equilibrium study of the system K_2CO_3, CO_2, $KHCO_3$ and water, Bur. Min. Rep. Invest. 23 (1959) 54–84.
[19] G. Astarita, A Gas Treating with Chemical Solvent, Wiely, New York, 1983.
[20] D.W. Van Krevelen, P. Hoftijzer, Kinetics of simultaneous absorption and chemical reaction, Chem. Eng. Prog. 44 (1948) 529–534.
[21] D.W. Savage, G. Astarita, S. Joshi, Chemical absorption and desorption of carbon dioxide from hot carbonate solutions, Chem. Eng. Sci. 35 (1980) 1513–1522.
[22] R.C. Reid, J.M. Prausnitz, T.K. Sherwood, The properties of Gases and Liquids, McGraw-Hill, New York, 1977.
[23] G.P. Bocard, B.J. Maryland, Investigation of the equilibrium between vapor, carbon dioxide and hot potassium carbonate solutions, Hydrol. Proc. Petrol. Refinery 41 (1962) 128–135.
[24] A.L. Kohl, F.C. Risenfield, Gas purification, Houston, TX, Gulf, 1985.
[25] L. Fox, Numerical Solution of Two-Point Boundary Problems in Ordinary Differential Equation, Oxford University Press, Oxford, London, 1957.
[26] H.B. Keller, Numerical Method for Two-Point Boundary Value Problems, Blaisdell, Walthams, MA, 1968.
[27] S.M. Roberts, J.S. Shipman, Two-Point Boundary Value Problems: Shooting Methods, American Elsevier, New York, 1972.